CHAPTER IV

RESULTS AND DISCUSSION

1. The isoquinoline alkaloids from the nudibranch *Jorunna funebris*

1.1 Extraction and isolation of the isoquinoline alkaloids

J. funebris (20 animals; 500 g, wet weight) was collected in the vicinity of Sichang Island at the depth of 3-5 meters in March 2004 and the egg ribbons (23.2 g, wet weight) were separately obtained in November 2004. The animals were carefully dissected into two parts, the mantles and the visceral organs (the combined digestive tracts and gonads). Then, each part was separately homogenized with phosphate buffer (pH 7) and 10% KCN solution. After 5 h, the mixture was repeatedly macerated with methanol, and then the extract was filtered and concentrated. The concentrated filtrate was partitioned between ethyl acetate and water, and the organic layer was concentrated *in vacuo* to give the residue (from the mantles, 700 mg; the visceral organs, 980 mg; and the egg ribbons, 270 mg). Each residue was separately subjected to flash column chromatography on silica gel to give isoquinoline-type compounds, as summarized in Table 9.

Table 9 Amount (mg) of isoquinoline marine natural products isolated from the nudibranch *J. funebris* pretreated with KCN.

Part	Jorunnamycins			Renieramycins				Mimosamycin
	A	B	C	M	N	O	Q	
Mantles	7.5	0	0	**25.3**	0.5	6.4	0	1.0
Visceral organs	0	**23.6**	0	0	9.2	2.0	1.3	9.0
Egg ribbons	3.8	0	**21.7**	**62.1**	0	0	0	0

1.2 Distribution of the isoquinoline alkaloids in the nudibranch *J. funebris*

Three new stabilized bistetrahydroisoquinoline compounds, including jorunnamycins A, B, and C were isolated from *J. funebris* along with five known compounds, including renieramycins M, N, O, and Q, and mimosamycin. Jorunnamycin A, the deangeloylrenieramycin M, was found both in the mantles and the egg ribbons while it was absent in the visceral organs. Jorunnamycin B was only found in the visceral organs as the major components while jorunnamycin C was only present in the egg ribbons as one of the main components. Interestingly, these three new compounds have never been reported from the sponge *Xestospongia* sp. which is the main food of the nudibrach *J. funebris*. However, the renieramycins existing in the sponge *Xestospongia* sp. including renieramycins M, N, O, and Q were also isolated from the nudibranch. Renieramycin M, the major renieramycin in the sponge, was found in both the mantles and the egg ribbons as the major compounds as well but absent in the visceral organs. Renieramycins N and O together with the monomeric isoquinoline, mimosamycin, were found both in the mantles and the visceral organs while renieramycin Q was found only in the visceral organs as the minor component.

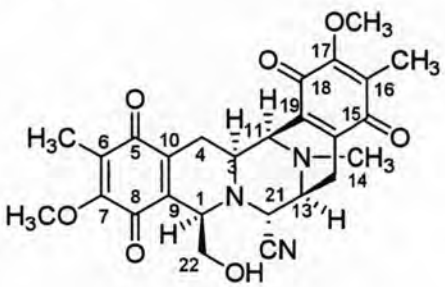

jorunnamycin A

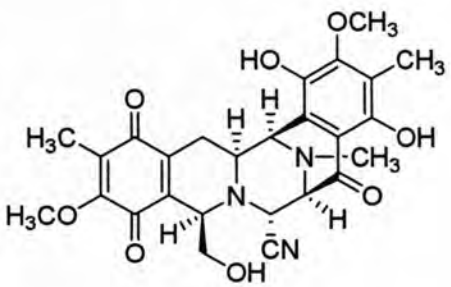

jorunnamycin B

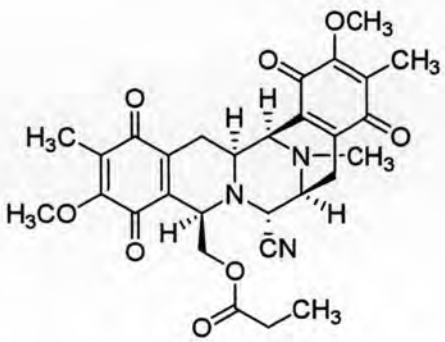

jorunnamycin C

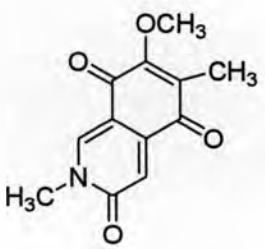

mimosamycin

Field observations during our collection trips around Sichang Island revealed that the nudibranch *J. funebris* fed on only the blue sponge *Xestospongia* sp. This behavior suggested that the nudibranch could sequester secondary metabolites from the sponge. Many reports have indicated that the sequestered secondary metabolites demonstrate predator-prey relationships between the predator nudibranchs and the prey sponges, and nudibranchs subsequently survive from their predators (Avila *et al.*, 1990; Proksh, 1994). In our case, renieramycin M, which might exist as renieramycin E in nature, was found to be the major component in both the mantles and the egg ribbons of the nudibranch as well as in the sponge tissues. Both renieramycin M and renieramycin E were reported to show strong cytotoxicity against tumor cell lines as well as antimicrobial activity (Saito *et al.*, 2004). As the mantles and the egg ribbons are the most vulnerable part to be attacked by predators and microorganisms, the nudibranch might be expected to sequester mainly renieramycin E from the *Xestospongia* sponge and then transfer to these tissues to support its putative defensive mechanism against predators. Interestingly, the stabilized jorunnamycins A-C have not been isolated from the sponge *Xestospongia* sp. pretreated with KCN, therefore the nudibranch might hydrolyze the angelic acid ester into the corresponding carbinolamine analog. On the other hand, the corresponding carbinolamine analog of jorunnamycin A was further converted into the corresponding carbinolamine analog of jorunnamycin C in the nudibranch. Incubation of jorunnamycin C with aqueous 10% KCN solution in methanol at room temperature for one week and further HPLC analysis of the solution completely revealed the absence of jorunnamycin A. The result ruled out the possibility of jorunnamycin A as the hydrolysis product of jorunnamycin C during the extraction process. Mimosamycin was also found mainly in the visceral organs. Thus, the chemical modification in the nudibranch might involve enzymatic transformation or oxidative degradation of bistetrahydroisoquinolinequinones into simple isoquinolinequinones. Further studies to clarify the ecological role are needed regarding the distribution of these compounds in the nudibranch.

1.3 Structure elucidation of the isolated isoquinoline alkaloids

The structures of the isolated compounds were characterized according to analyses of their spectroscopic data including MS, IR, UV, CD, optical rotation, and NMR spectroscopy together with literature data comparison.

1.3.1 Structure elucidation of jorunnamycins A-C

Three new compounds, jorunnamycins A, B, and C were isolated, and their NMR data were very characteristic of renieramycin-type marine natural products.

1.3.1.1 Jorunnamycin A

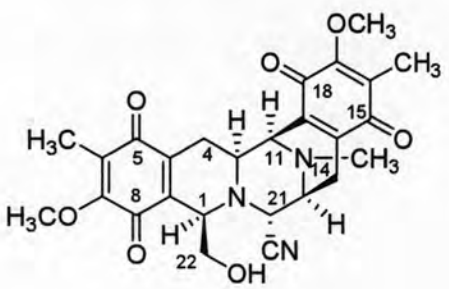

jorunnamycin A

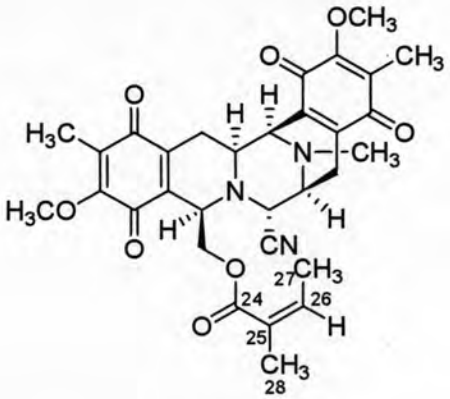

renieramycin M

Jorunnamycin A was obtained as a pale yellow amorphous solid. The compound showed a large negative optical rotation at -270.6 (c = 1.0, $CHCl_3$) similar to other bistetrahydroisoquinolinequinone renieramycins (Suwanborirux *et al.*, 2003 and Amnuoypol *et al.*, 2004). The molecular formula $C_{26}H_{27}N_3O_7$ was deduced on the basis of HR-FABMS showing the pseudomolecular ion peak $[M+H]^+$ at *m/z* 494.1910. The UV spectrum of jorunnamycin A (Figure 8) displayed the quinone absorption at λ_{max} (log ε) at 269 (4.26) nm. The circular dichroism (CD) spectrum of jorunnamycin A was shown in the Figure 9. The IR spectrum revealed the absorption band at 1656 cm^{-1} (C=O stretching) implying the quinone character of jorunnamycin A (Figure 10). Complete proton and carbon assignments of jorunnamycin A were achieved by interpretation of the data obtained from 1D-NMR and 2D-NMR as shown in Table 10.

The 500 MHz ^{1}H NMR spectrum of jorunnamycin A in $CDCl_3$ (Figure 11) exhibited the presence of two methoxy groups at δ 3.98 and 4.03 ppm (7-OCH_3 and 17-OCH_3), three groups of methylene protons at δ 1.42 ppm (1H, ddd, J = 17.4, 11.6, 2.4 Hz, 4-Hβ); 2.27 ppm (1H, d, J = 21.1 Hz, 14-Hβ); 2.82 ppm (1H, dd, J = 21.1, 7.6 Hz, 14-Hα); 2.92 ppm (1H, dd, J = 17.4, 2.4 Hz, 4-Hα); 3.48 ppm (1H, dd, J = 11.3, 3.7 Hz, 22-Hb); 3.71 ppm (1H, dd, J = 11.3, 3.1 Hz, 22-Ha), five methine protons at δ 3.17 ppm (1H, ddd, J = 11.6, 2.6, 2.4 Hz, 3-H); 3.41 ppm (1H, dd, J = 7.6, 2.4 Hz, 13-H); 3.89 ppm (1H, ddd, J = 3.7, 3.1, 2.4 Hz, 1-H); 4.07 ppm (1H, d, J = 2.6 Hz, 11-H); 4.15 ppm (1H, d, J = 2.4 Hz, 21-H), and three methyl proton signals at δ 2.30 (3H, s, 12-NCH_3) and 1.93 ppm (6H, s, 6-CH_3 and 16 CH_3).

The 125 MHz ^{13}C NMR spectrum of jorunnamycin A in $CDCl_3$ (Figure 13) displayed twenty-six carbon signals. The DEPT-90 and DEPT-135 (Figure 14) and HMQC (Figures 15-16) spectra of jorunnamycin A were used to classify the type of carbons and their connectivity with nearby protons. These experiments indicated two methoxy carbons at δ 61.0 ppm and 61.1 ppm, two methyl carbons connecting to double bond (δ 8.7 ppm) and one downfield methyl carbon connecting to a nitrogen (δ 41.5 ppm), three methylene carbons (δ 21.5, 25.4 and δ 64.2), five methine carbons (δ 54.2, 54.3, 54.5, 58.1, and 59.1 ppm), and thirteen quaternary carbons. One quaternary carbon signal at δ 116.9 ppm was the cyano carbon at C-21. The downfield quaternary carbon signals at δ 155.4 ppm (C-17) and 155.7 ppm (C-7) appeared to be those of oxygenated carbons. The most downfield carbon signals at δ 181.4 ppm (C-8), 182.3 ppm (C-18), 185.5 ppm (C-5), and 186.3 (C-15) were carbonyl carbons of the two quinone rings.

The ^{1}H-^{1}H COSY spectrum of jorunnamycin A (Figure 12) revealed the correlations of coupled protons as follows: H-21 (δ 4.15 ppm) was coupled with H-13 (δ 3.41 ppm) with J = 2.4 Hz of vicinal coupling; H-3 (δ 3.17 ppm) was coupled with H-11 (δ 4.07 ppm) with J = 2.6 Hz of vicinal coupling and was also vicinal coupled with H-4α (δ 2.92 ppm) with J = 2.4 Hz and H-4β (δ 1.42 ppm) with J = 11.6 Hz; H-4α (δ 2.92 ppm) was geminal coupled with H-4β (δ 1.42 ppm) with J = 17.4 Hz; H-22a (δ 3.71 ppm) was geminal coupled with H-22b (δ 3.48 ppm) with J = 11.3 Hz; H-14α (δ 2.82 ppm) was geminal coupled with H-14β (δ 2.27 ppm) with J = 21.1 Hz and vicinal coupled with H-13 (δ 3.41ppm) with J = 7.6 Hz; H-1 (δ 3.89 ppm) was

coupled with H-22a (δ 3.71 ppm) with J = 3.1 Hz and H-22b (δ 3.48 ppm) with J = 3.7 Hz of vicinal coupling and homoallylic coupled with H-4β with J = 2.4 Hz.

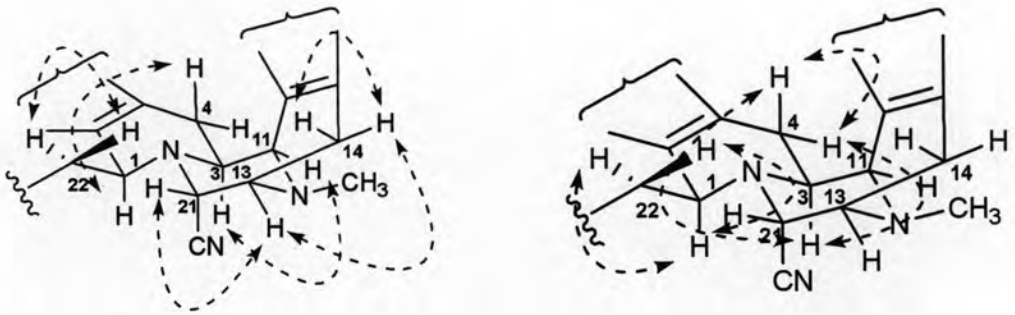

◄----► = H-H correlations in the ^{1}H-^{1}H COSY spectrum of jorunnamycin A

The chemical structure of jorunnamycin A was finally accomplished by the HMBC spectrum ($^nJ_{HC}$ = 8 Hz) (Figures 17-20). The assignments of protons and carbons and long-range correlations of jorunnamycin A are summarized in Table 10.

The substituents of ring A were assigned as follows: a methyl group was located on C-6 based on ^{1}H-^{13}C long-range correlations between the 6-CH_3 protons and C-5, C-6, and C-7. A methoxy group was attached to C-7 based upon long-range correlation of the 7-OCH_3 protons to C-7. Connection between ring A and ring B was confirmed by HMBC correlations observed between 1-H, 4-Hα, 4-Hβ, and 22-Ha to C-9 and 1-H, 4-Hα, and 4-Hβ to C-10. Moreover, 4-Hα also displayed long-rang correlation to C-5.

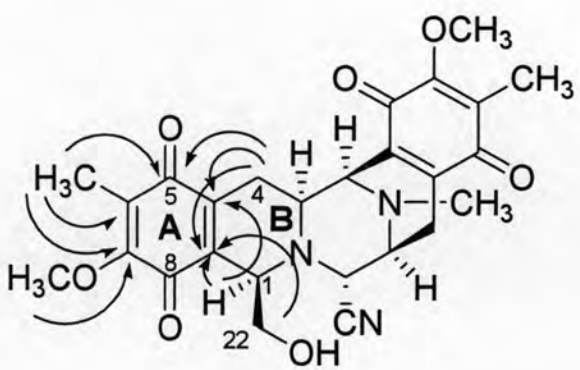

⟶ = H to C correlation in the HMBC spectrum of jorunnamycin A

The B and C rings were formed by insertion of a nitrogen atom between C-1, C-3 and C-21. The connection between both rings was confirmed by long-range correlations of 21-H to C-1 and C-3, 4-Hβ to C-11 and 1-H to C-21.

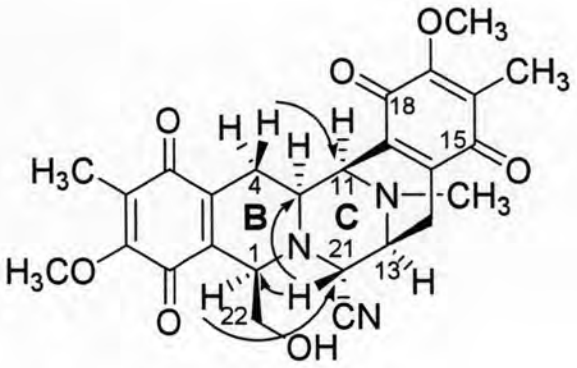

⟶ = H to C correlation in the HMBC spectrum of jorunnamycin A

The C and D rings were also formed by insertion of a nitrogen atom between C-11 and C-13. The connectivity was confirmed by the HMBC correlations between 14-Hα, 14-Hβ, and 13-H to C-21, 13-H and N-CH_3 to C-11, 11-H, 14-Hα, 14-Hβ, and N-CH_3 to C-13, and 13-H to 21-CN. The 21-H showed ^{1}H-^{13}C long-range correlation to 21-CN.

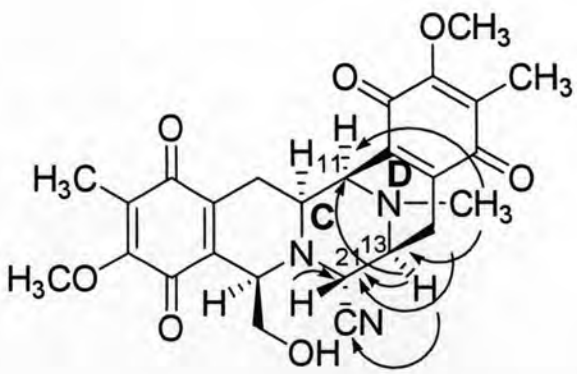

⟶ = H to C correlation in the HMBC spectrum of jorunnamycin A

The quinone E ring was connected to D ring based on the long-range correlations between 14-Hβ to C-15, 11-H and 14-Hβ to C-18, C-19, and C-20, 3-H, 13-H, and 14-Hα to C-19 and C-20. The substituents on ring E were assigned as follows: a methyl group was attached at C-16 base on HMBC correlation of 16 CH_3

proton to C-15, C-16, and C-17. A methxoxy group was located to C-17 based upon long-range correlation of the 17-OCH_3 protons to C-17, whereas C-18 was confirmed by the correlations from H-11 and 14-Hβ to C-18.

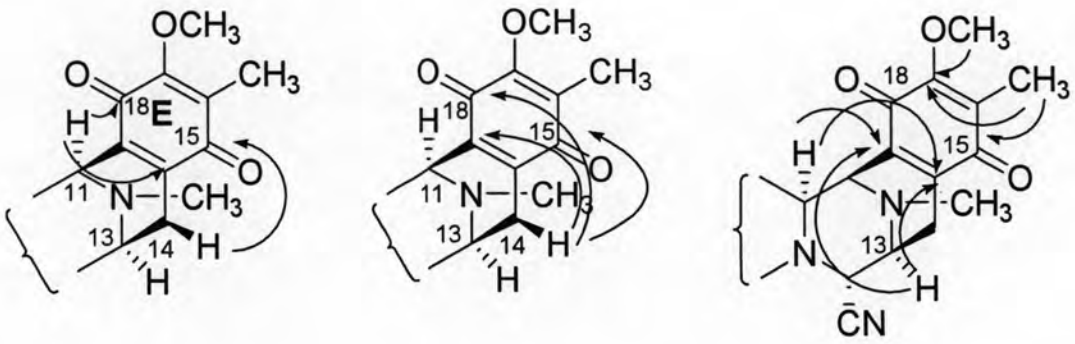

⟶ = H to C correlation in the HMBC spectrum of jorunnamycin A

The NMR data of jorunnamycin A are almost identical to those of renieramycin M except the angelate signals [δ_H 5.96/δ_C 140.5 (H-26), δ_H 1.82/δ_C 15.7 (CH_3-27), δ_H 1.58/δ_C 20.4 (CH_3-28), δ_C 166.5 (C-24), and δ_C 126.3 (C-25)] (Suwanborirux *et al.*, 2003). In addition, the methylene proton signals at C-22 of jorunnamycin A shifted upfield to δ_H 3.48 and 3.71 ppm when compared with those of renieramycin M (δ_H 4.10 and 4.53 ppm) from the literature (Suwanborirux *et al.*, 2003). Therefore, its structure was identical to deangeloylrenieramycin M, which was previously semisynthesized from hydrogenation and reduction of renieramycin M (Saito *et al.*, 2004). This is the first natural occurrence of jorunnamycin A.

Table 10 ^{1}H NMR, ^{13}C NMR, HMBC and NOESY assignments for jorunnamycin A in $CDCl_3$.

Position	δ_C (ppm)	δ_H (ppm), mult. (*J* in Hz)	HMBC correlations	NOESY correlations
1	58.1	3.89 (1H, ddd, 3.7, 3.1, 2.4)	21-H	21-H, 22Hb
3	54.3	3.17 (1H, ddd, 11.6, 2.6, 2.4)	11-H, 21-H	11-H
4	25.4	α 2.92 (1H,dd, 17.4, 2.4) β 1.42 (1H, ddd, 17.4, 11.6, 2.4)	-	4-Hβ 4-Hα
5	185.5	-	4-Hα, 6-CH_3	-
6	[a]128.8	-	6-CH_3	-
7	[b]155.7	-	6-CH_3, 7-OCH_3	-
8	181.4	-	-	-
9	136.1	-	1-H, 4-Hα, 4-Hβ, 22-Ha	-
10	141.4	-	1-H, 4-Hα, 4-Hβ	-
11	54.2	4.07 (1H, d, 2.6)	4-Hβ, 13-H, N-CH_3	N-CH_3
13	54.5	3.41 (1H, dd, 7.6, 2.4)	N-CH_3, 11-H, 14-Hα, 14-Hβ	N-CH_3,14-Hα, 14-Hβ 21-H
14	21.5	α 2.82 (1H, dd, 21.1, 7.6) β 2.27 (1H, d, 21.1)	-	14-Hβ 14-Hα
15	186.3	-	16-CH_3, 14-Hβ	-
16	[a]128.6	-	16-CH_3,	-
17	[b]155.4	-	16-CH_3, 17-OCH_3	-
18	182.3	-	11-H, 14-Hβ	-
19	135.6	-	3-H, 11-H, 14-Hα,14-Hβ	-
20	141.7	-	11-H, 13-H, 14-Hα, 14-Hβ	-
21	59.1	4.15 (1H, d, 2.4)	1-H, 13-H, 14-Hα, 14-Hβ	14-Hβ, 22-Ha
22	64.2	a 3.71 (1H, dd, 11.3, 3.1) b 3.48 (1H, dd, 11.3, 3.7)	-	22-Hb 22-Ha
6-CH_3	8.7	1.93 (3H, s)	-	-
16-CH_3	8.7	1.93 (3H, s)	-	-
7-OCH_3	[c]61.1	3.98 (3H, s)	-	-
17-OCH_3	[c]61.0	4.03 (3H, s)	-	-
N-CH_3	41.5	2.30 (3H, s)	11-H, 13-H	-
CN	116.9	-	21-H, 13-H	-

[a, b, c] interchangeable between these positions

1.3.1.2 Jorunnamycin B

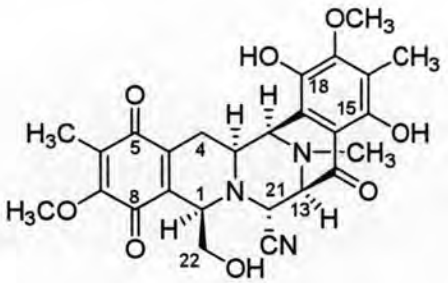

jorunnamycin B

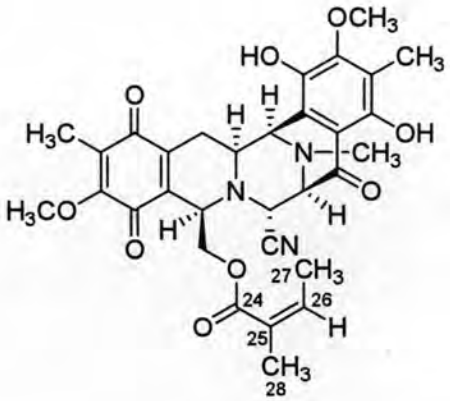

renieramycin Q

Jorunnamycin B was isolated as a yellowish orange amorphous solid showing positive optical rotation, $[\alpha]^{20}_{D}$ = +117.6 (*c* = 0.11, $CHCl_3$) different from other renieramycins. The HR-FABMS of jorunnamycin B showing the pseudomolecular ion peak $[M+H]^+$ at *m/z* 510.1877 established the molecular formula of $C_{26}H_{27}N_3O_8$, which was 16 mass units higher than that of jorunnamycin A. The UV spectrum (Figure 23) showed maximum absorption bands, λ_{max} (log ε), 254 (3.96), 275 (4.15), 371 (3.64) nm. The IR spectrum also exhibited absorption bands for hydroxyls 3436 cm^{-1} (broad) and for quinone carbonyls at 1656 and 1639 cm^{-1} (Figure 25).

The 300 MHz ^1H NMR spectrum (Figure 26) of jorunnamycin B showed signals for two groups of methoxy protons at δ 3.85 ppm (17-CH_3) and 3.96 ppm (7-CH_3), *N*-methyl protons at δ 2.44 (12-NCH_3), and two groups of aromatic methyl protons appearing as two singlets at δ 1.90 ppm (6-CH_3) and 2.17 ppm (16-CH_3). Five downfield methine proton signals revealed at δ 4.37 ppm (11-H), 4.33 ppm (21-H), 3.90 (1-H), 3.44 (13-H), and 3.35 (3-H) which were on the carbons connecting to nitrogen atoms. From the previous data, jorunnamycin A exhibited three sp^3 methylene proton signals whereas the ^1H NMR spectrum of this compound showed only two groups of sp^3 methylene proton signals at δ 1.64 ppm (1H, ddd, *J* = 17.9, 11.4, 2.4 Hz, 4-Hβ); 3.08 ppm (1H, dd, *J* = 17.9, 2.5 Hz, 4-Hα); 3.35 ppm (1H, d, *J* = 11.5 Hz, 22-Hb); 3.61 ppm (1H, dd, *J* = 11.5, 3.0 Hz, 22-Ha). The methylene proton signals at C-14 were absent. Moreover, the signals of two phenolic hydroxyl protons

displayed at δ 5.80 ppm (18-OH) and 11.46 ppm (15-OH). Both OH signals were disappeared in the presence of deuterium dioxide (D_2O).

Analyses of the 75 MHz ^{13}C NMR (Figure 28) and DEPT-135 (Figure 29) NMR spectra revealed that compound jorunnamycin B contained two methyl carbons connecting to double bonds at δ 8.9 ppm (6-CH_3) and δ 9.1 ppm (16-CH_3); an *N*-methyl carbons at δ 42.7 ppm (12-NCH_3); two methoxy carbons at δ 61.1 ppm (7-OCH_3) and at δ 61.5 ppm (17-OCH_3). Two methylene carbon signals appeared at δ 24.0 ppm (C-4) and 63.5 ppm (C-22), whereas five methine carbons at δ 53.7 (C-3), 56.7 (C-11 and C-21), 57.6 (C-1), and 65.9 (C-13) were observed. There were thirteen quaternary carbon signals in ^{13}C NMR spectrum, of which the most upfield quaternary carbon signal at δ 115.4 ppm (21-CN) was that of an sp carbon connected to a nitrogen atom. The downfield quaternary carbon signals at δ 139.9 (C-18), 155.0 (C-15), 154.0 (C-17), 155.3 (C-7), 180.9 (C-8), 185.3 (C-5), and 197.4 (C-14) were assignable to oxygenated sp^2 carbons. The carbon signals at δ 111.4 (C-20), 116.4 (C-19), 119.3 (C-16), 128.5 (C-6), 135.8 (C-9), 141.1 (C-10) were defined as un-oxygenated sp^2 quaternary.

From the ^1H-^1H COSY (Figure 27) and HMQC (Figure 30) spectra, all protonated carbons could be assigned. The HMBC experiment (Figures 31-33) showed long range correlations between ^1H-^{13}C signals, which helped in assigning the carbon positions of jorunnamycin B as shown in Table 11.

Interestingly, the ^{13}C NMR data showed two carbonyl resonances (δ 185.3 and 180.9 ppm) of a quinone ring and an unsaturated ketone carbonyl resonance at δ 197.4 ppm. The ^1H-NMR revealed characteristic D_2O exchangeable protons (δ 11.46 and 5.80 ppm). Moreover, the diagnostic homoallylic coupling (2.4 Hz) between 1-H and 4-Hβ through five bonds confirmed the presence of the quinone ring at the A ring These data revealed that the quinone rings at the E ring of jorunnamycin A was reduced to form the hydroquinone ring with the pericarbonyl function (C-14), similar to renieramycin Q (Amnuoypol *et al.*, 2004) and cribrostatin 4 (Parameswaran *et al.*, 1998, Pettit *et al.*, 2000; Saito *et al.*, 2001). However, the characteristic NMR signals for the angeloyl side chain in renieramycin Q [δ_H 5.81/δ_C 139.6 (H-26), δ_H 1.68/δ_C 15.4 (CH_3-27), δH 1.54/δC 19.8 (CH_3-28), δ_C 166.6 (C-24), and δ_C 126.5 (C-25)] were absent in jorunnamycin B. In addition, the upfield shifts to δ_H 3.35 and 3.61 ppm of

the methylene protons of jorunnamycin B when compared with those of renieramycin Q (δ_H 4.02 and 4.09 ppm) confirmed the free alcohol functionality at C-22. Therefore, jorunnamycin B was determined as deangeloylrenieramycin Q.

Table 11 ^{1}H NMR, ^{13}C NMR, HMBC and NOESY assignments for jorunnamycin B in $CDCl_3$.

Position	δ_C (ppm)	δ_H (ppm), mult. (*J* in Hz)	HMBC Correlations	NOESY correlations
1	57.6	3.90 (1H, overlapped)	-	21-H
3	53.7	3.35 (1H, dt, 11.4, 2.7)	4-Hβ, 11-H	11-H
4	24.0	α 3.08 (1H, dd,17.9,2.5) β 1.64 (1H, ddd, 17.9, 11.4, 2.4)	-	4-Hβ 4-Hα
5	185.3	-	4-Hα, 6-CH_3	-
6	128.5	-	6-CH_3	-
7	155.3	-	6-CH_3, 7-OCH_3	-
8	180.9	-	-	-
9	135.8	-	3-H, 4-Hα, 4-Hβ, 22-Ha	-
10	141.1	-	4-Hα, 4-Hβ	-
11	56.7	4.37 (1H, br s)	N-CH_3	3-H, N-CH_3
13	65.9	3.44 (1H, br s)	N-CH_3	N-CH_3
14	197.4	-	13-H, 15-OH	-
15	155.0	-	15-OH	-
16	119.3	-	16-CH_3, 15-OH	-
17	154.0	-	16-CH_3, 17-OCH_3	-
18	139.9	-	-	-
19	116.4	-	-	-
20	111.4	-	15-OH, 11-H	-
21	56.7	4.33 (1H, d, 2.6)	-	1-H, 13-H, 22-Ha
22	63.5	a 3.61 (1H, dd, 11.5, 3.0) b 3.35 (1H, d, 11.5)	-	22-Hb 22-Ha
6-CH_3	8.9	1.90 (3H, s)	-	-
16-CH_3	9.1	2.17 (3H, s)	-	17-OCH_3
7-OCH_3	61.1	3.96 (3H, s)	6-CH_3	-
17-OCH_3	61.5	3.85 (3H, s)	16-CH_3	-
N-CH_3	42.7	2.44 (3H, s)	-	-
CN	115.4	-	21-H	-
15-OH	-	11.46 (1H, s)	-	-
18-OH	-	5.80 (1H, s)	-	-

1.3.1.3 Jorunnamycin C

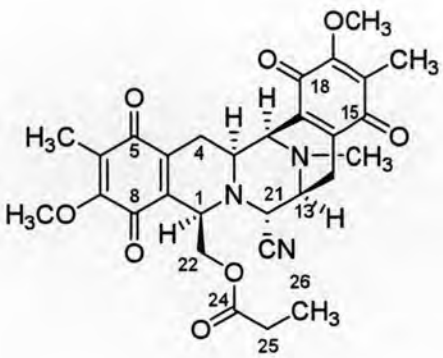

jorunnamycin C

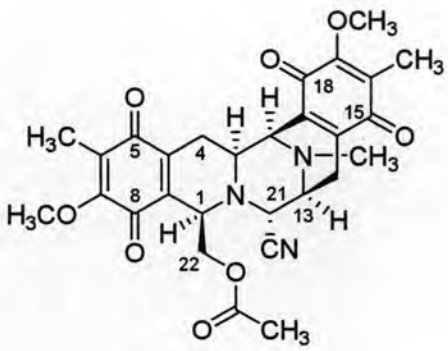

21-cyanojorumycin

Jorunnamycin C was isolated as a yellow amorphous solid, $[\alpha]^{20}_{D}$ = -91.6 (*c* = 0.1, $CHCl_3$). The molecular formula of jorunnamycin C was determined to be $C_{29}H_{31}N_3O_8$ on the basis of high-resolution EIMS, and it was 14 mass units higher than that of the 21-cyanojorumycin, which was previously prepared from deangeloylrenieramycin M and acetyl chloride (Saito *et al.*, 2004). The UV spectrum of jorunnamycin C displayed maximum absorptions at λ_{max} (log ε), 268 (4.25), 347 (3.14) nm (Figure 36). The IR spectrum (Figure 38) revealed the absorption bands at ν_{max} 1736 cm^{-1} implied the ester carbonyl.

The 500 MHz ^{1}H NMR spectrum of jorunnamycin C in $CDCl_3$ (Figure 39) revealed the signals attributable to an *N*-methyl signal at δ 2.29 ppm (12-NCH_3), two olefinic methyl groups appearing as two singlets at δ 1.95 ppm (6-CH_3 and 16-CH_3). Two methoxy groups were presented as two singlets at δ 4.01 ppm (17-OCH_3 and 7-OCH_3). The ^{1}H-NMR spectrum also showed signals for three sp^3 methylene groups at δ 2.93 ppm (1H, dd, *J* = 17.1, 2.4 Hz, 4-Hα) and 1.31 ppm (1H, ddd, *J* = 17.1, 11.6, 2.4 Hz, 4-Hβ); δ 2.76 ppm (1H, dd, *J* = 21.1, 7.6 Hz, 14-Hα) and 2.31 (1H, d, *J* = 21.1 Hz, 14-Hβ); 4.40 ppm (1H, dd, *J* = 11.6, 3.2 Hz, 22-Ha) and 3.89 (1H, dd, *J* = 11.6, 4.0 Hz, 22-Hb). Five sp^3 methine proton signals were revealed at δ 3.10 ppm (H-3), 3.37 ppm (H-13), 3.99 ppm (H-1), 4.02 ppm (H-11), 4.07 ppm (H-21). Moreover, jorunnamycin C showed the characteristic ^{1}H NMR signals of the propionate at δ 2.11, 2.02 (1H, each, dq, 16.5, 7.6 Hz, 25-H_2) and 0.95 (3H, t, *J* = 7.6 Hz, 26-H_3).

The 125 MHz ^{13}C NMR spectrum of jorunnamycin C in $CDCl_3$ (Figure 41) exhibited twenty-nine carbon signals. Classification of these carbon signals by DEPT-135, DEPT-90 (Figure 42), and HMQC (Figure 43) indicated the presence of the signals for three methyl carbons at δ 8.6 (6-CH_3), 8.8 (16-CH_3), and 8.9 (C-26); an *N*-methyl carbon at δ 41.5 ppm (12-NCH_3); two methoxy carbons at δ 61.0 and 61.1 ppm (7-OCH_3 and 17-OCH_3). Three upfield sp^3 methylene carbons appeared at δ 21.2 ppm (C-14), 25.3 ppm (C-4) and 27.4 (C-25), whereas an one downfield sp^3 methylene at δ 63.6 ppm was assigned at C-22 connecting oxygen of an ester group. Five sp^3 methine carbon showed at δ 54.3 (C-11), 54.5 ppm (C-3), 54.6 (C-13), 55.9 (C-1), and 59.0 (C-21). There were fourteen quaternary carbon signals in the ^{13}C NMR spectrum. The downfield quaternary carbon signals at δ 155.2 (C-17), 155.6 ppm (C-7), 173.4 ppm (C-24), 180.9 ppm (C-8), 182.4 (C-18), 185.4 ppm (C-5), and 186.2 ppm (C-15) were assignable to oxygenated sp^2 carbons. The carbon signals at δ 128.6 ppm (C-16), 128.6 (C-6), 135.0 (C-19), 135.5 (C-9), 141.7 (C-10), and 142.1 (C-20) were defined as un-oxygenated sp^2 quaternary carbons. The quaternary carbon of cyanide (21-CN) at δ 116.9 ppm was also present.

From the information above, the structure of jorunnamycin C is related to renieramycin M except for the presence of the propionic acid ester at δ_C 173.4 ppm ($O\underline{C}OCH_2CH_3$); δ_H 2.11, 2.02 ppm and δ_C 27.4 ppm ($OCO\underline{CH_2}CH_3$); and δ_H 0.95 ppm and δ_C 8.9 ppm ($OCOCH_2\underline{CH_3}$) instead of the angelate ester of renieramycin M.

From the ^1H-^1H COSY (Figure 40) and HMBC (Figures 44-46) data, jorunnamycin C showed similar patterns with renieramycin M. The attached propionate group to C-24 was confirmed by ^1H-^{13}C long-range correlation between 25-H_2 and 26-H_3 to C-24.

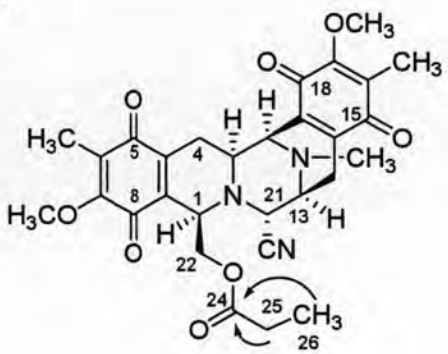

⟶ = H to C correlation in the HMBC spectrum of jorunnamycin C

Table 12 ^{1}H NMR, ^{13}C NMR, HMBC and NOESY assignments for jorunnamycin C in $CDCl_3$.

Position	δ_C (ppm)	δ_H (ppm), mult. (*J* in Hz)	HMBC Correlations	NOESY Correlation□
1	55.9	3.99 (1H, d, 2.4)	22-Ha	22-Ha
3	54.5	3.10 (1H, ddd, 11.6, 2.7, 2.5)	1-H, 21-H	11-H
4	25.3	α 2.93 (1H, dd, 17.1, 2.4) β 1.31 (1H,ddd, 17.1, 11.6, 2.4)	-	4-Hβ 4-Hα
5	185.4	-	4-Hα, 6-CH_3	-
6	128.6	-	6-CH_3	-
7	155.6	-	7-OCH_3, 6-CH_3	-
8	180.9	-	-	-
9	135.5	-	1-H, 4-Hα, 4-Hβ, 22-Ha, b	-
10	141.7	-	4-Hα ,4- Hβ, 13-H	-
11	54.3	4.02 (1H,d, 2.7)	4-Hα , 4-Hβ, 13-H, N-CH_3	N-CH_3
13	54.6	3.37 (1H ,d, 2.2)	14-Hα, 14-Hβ	21-H, N-CH_3
14	21.2	α 2.76 (1H, dd, 21.1, 7.6) β 2.31 (1H, d, 21.1)	13-H, 21-H	13-H, 14-Hβ, 14-Hα, 21-H
15	186.2	-	14-Hα, 14-Hβ, 16-CH_3, N-CH_3	-
16	128.6	-	16-CH_3	-
17	155.2	-	17-OCH_3, 16-CH_3	-
18	182.4	-	11-H	-
19	135.0	-	3-H, 14-Hα, 14-Hβ	-
20	142.1	-	11-H, 13-H, 14-Hα, 14-Hβ	-
21	59.0	4.07 (1H, dd, 2.4)	13-H, 14-Hα, 14-Hβ	14-Hβ, 22-Ha
22	63.6	a 4.40 (1H, dd, 11.6, 3.2) b 3.89 (1H, dd, 11.6, 4.0)	-	21-H 22-Ha
24	173.4	-	22-Ha, b, 25-H_2, 26-H_3	-
25	27.4	2.11, 2.02 (1H each, dq, 16.5, 7.6)	26-H_3	26-H_3
26	8.9	0.95 (3H, t, 7.6)	25-H_2	25-H_2
6-CH_3	8.6	1.95 (3H, s)	-	-
16-CH_3	8.8	1.95 (3H, s)	-	-
7-OCH_3	61.0	4.01 (3H, s)	-	-
17-OCH_3	61.1	4.01 (3H, s)	-	-
N-CH_3	41.5	2.29 (3H, s)	13-H, 11-H	-
CN	116.9	-	13-H, 21-H	-

The relative configurations at C-1, C-3, C-4, C-11 of jorunnamycins A-C were deduced from NOESY experiments (Figures 21, 34, and 47). The NOE correlations of 1-H/3-H/11-H/13-H confirmed the α-orientation of those protons in the molecule. The NOE correlations between 14-Hβ and 21-Hβ revealed the relative stereochemistry at C-21 of jorunnamycins A and C.

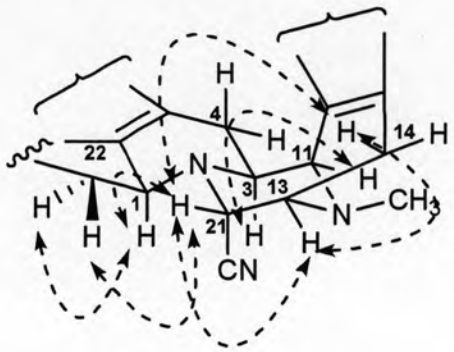

Jorunnamycin A

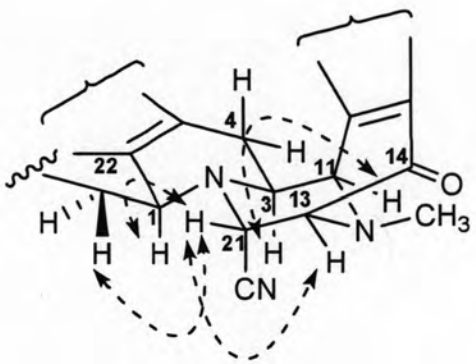

Jorunnamycin B

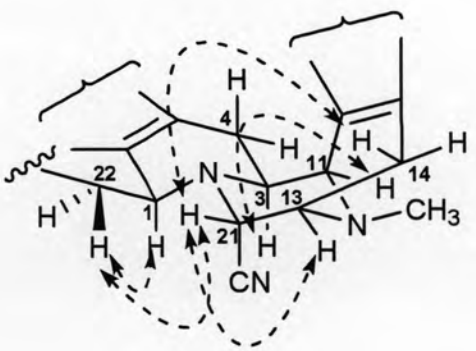

Jorunnamycin C

◄- - ► = NOE correlations

Interestingly, jorunnamycin A showed a large negative optical rotation at -270.6 (c = 1.0, $CHCl_3$) and on the other hand, jorunnamycin B revealed positive optical rotation, $[\alpha]^{20}_D$ = +117.6 (c = 0.11, $CHCl_3$). The difference of these optical rotations might be the result from an oxygen substitute at C-14 and a dihydroquinone at ring E of jorunnamycin B

1.3.2 Structure elucidation of the known compounds, renieramycins M, N, O, and Q and mimosamycin

The known metabolites including renieramycins M, N, O, and Q and mimosamycin were identified by comparing their ^1H NMR and ^{13}C NMR data with those of authentic standards and with the literature values (Suwanborirux *et al.*, 2003; Amnuoypol *et al.*, 2004). Renieramycins M, N, O, and Q have been previously isolated from the Thai blue sponge *Xestospongia* sp. (Suwanborirux *et al.*, 2003; Amnuoypol *et al.*, 2004).

1.3.2.1 Renieramycin M

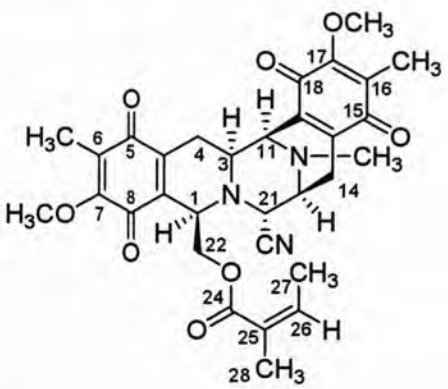

The ESI-TOF mass spectrum of renieramycin M showed a protonated molecular ion $[M+H]^+$ at m/z 576 implying a molecular formula of $C_{31}H_{33}N_3O_8$ (Figure 48). Renieramycin M was obtained as an orange amorphous solid. The proton and carbon NMR assignments were accomplished by comparison with previous data of renieramycin M (Suwanborirux *et al.*, 2003) as shown in Table 13.

The 300 MHz ^1H NMR spectrum of renieramycin M in $CDCl_3$ (Figure 49) exhibited the signals attributable to an *N*-methyl proton at δ 2.26 ppm (12-NCH_3), two aromatic methyl groups appearing as two singlets at δ 1.88 and 1.92 ppm (6-CH_3 and

16-CH_3). Two methoxy groups were present as two singlets at δ 4.00 ppm (17-OCH_3) and 3.97 ppm (7-OCH_3). The ^{1}H NMR also showed three groups of sp^3 methylene protons at δ 2.87 ppm (1H, dd, J = 17.4, 2.2 Hz, 4-Hα) and 1.35 ppm (1H, ddd, J = 17.4, 11.4, 2.6 Hz, 4-Hβ); δ 2.73 ppm (1H, dd, J = 21.1, 7.5 Hz, 14-Hα) and 2.28 (1H, d, J = 21.1 Hz, 14-Hβ); 4.51 ppm (1H, dd, J = 11.7, 2.9 Hz, 22-Ha) and 4.10 (1H, dd, J = 11.7, 2.6 Hz, 22-Hb). Five sp^3 methine proton signals at δ 3.09, 3.37, 3.99, 4.01, 4.05 ppm were assigned to 3-H, 13-H, 1-H, 11-H, and 21-H, respectively. Moreover, an angelate ester side chain revealed two methyl protons which connected double bond at δ 1.80 ppm (27-H_3) and 1.55 ppm (28-H_3) and one olefinic proton at δ 5.94 ppm.

The 75 MHz ^{13}C NMR spectrum of renieramycin M in $CDCl_3$ (Figure 50) indicated the presence of two methyl carbons connecting to double bonds at δ 8.6 (16-CH_3) and 8.9 (6-CH_3); an *N*-methyl carbon at δ 41.5 ppm (12-NCH_3); two methoxy carbons at δ 61.0 and 61.1 ppm (7-OCH_3 and 17-OCH_3). Two upfield sp^3 methylene carbons appeared at δ 21.5 and 25.5 ppm (C-14 and C-4); whereas an one downfield sp^3 methylene at δ 62.0 ppm was assigned C-22 which connected oxygen of ester carbonyl. Five sp^3 methine carbon showed at δ 54.0 ppm (C-3), 54.3 (C-11), 54.6 (C-13), 56.3 (C-1), and 58.3 (C-21) and one sp^2 methine carbon at δ 140.4 (C-26). There were fifteen quaternary carbons signals in the ^{13}C-NMR spectrum. The downfield quaternary carbon signals at δ 155.0 (C-17), 155.6 ppm (C-7), 166.3 ppm (C-24), 180.7 ppm (C-8), 182.0 (C-18), 185.1 ppm (C-5), and 185.5 ppm (C-15) were assignable to oxygenated sp^2 carbons. The carbon signals at δ 126.1 ppm (C-25), 128.3 ppm (C-16), 128.5 (C-6), 134.4 (C-19), 135.5 (C-9), 141.0 (C-10), and 141.9 (C-20) were defined as un-oxygenated sp^2 quaternary carbons. Moreover, quaternary carbon of cyanide (21-CN) at δ 116.7 ppm was also present.

Table 13 ^{1}H NMR and ^{13}C NMR assignments for renieramycin M in $CDCl_3$.

Position	δ_C (ppm)		δ_H (ppm), mult. (*J* in Hz)	
	Renieramycin M (75 MHz)	**Renieramycin M** (Suwanborirux *et al.*, 2003) (125 MHz)	**Renieramycin M** (300 MHz)	**Renieramycin M** (Suwanborirux *et al.*, 2003) (500 MHz)
1	56.3	56.3	3.99 (1H, overlap)	3.99 (1H, m)
3	54.0	54.1	3.09 (1H, ddd, 11.4, 2.7)	3.11 (1H, ddd, 11.3, 3.1, 2.8)
4	25.5	25.4	α 2.87 (1H, dd, 17.4, 2.2) β 1.35 (1H,ddd, 17.4,11.4, 2.6)	α 2.89 (1H, dd, 17.4, 2.8) β 1.36 (1H,ddd, 17.4,11.3, 2.7)
5	185.1	185.4	-	-
6	128.5	128.6	-	-
7	155.6	155.8	-	-
8	180.7	180.9	-	-
9	135.5	135.7	-	-
10	141.0	141.3	-	-
11	54.3	54.2	4.01 (1H,overlap)	4.01 (1H, d, 3.1)
13	54.6	54.6	3.37 (1H, d, 7.5)	3.40 (1H, ddd, 7.6 2.5, 1.8)
14	21.5	21.3	α 2.73 (1H, dd, 21.1, 7.5) β 2.28 (1H, d, 21.1)	α 2.76 (1H, dd, 20.6, 7.6) β 2.30 (1H, d, 20.6)
15	185.5	185.9	-	-
16	128.3	128.4	-	-
17	155.0	155.2	-	-
18	182.0	182.5	-	-
19	134.4	135.0	-	-
20	141.9	142.0	-	-
21	58.3	58.5	4.05 (1H, d, 2.3)	4.07 (1H, d, 2.5)
22	62.0	62.0	a 4.51 (1H, dd, 11.7, 2.9) b 4.10 (1H, dd, 11.7, 2.6)	a 4.53 (1H, dd, 11.6, 3.1) b 4.10 (1H, dd, 11.6, 2.5)
6-CH_3	8.6	8.5	1.88 (3H, s)	1.90 (3H, s)
16-CH_3	8.9	8.7	1.92 (3H,s)	1.94 (3H, s)
7-OCH_3	61.0	60.9	3.97 (3H, s)	3.99 (3H, s)
17-OCH_3	61.1	61.0	4.00 (3H, s)	4.02 (3H, s)

Table 13 (continued).

Position	δ_C (ppm)		δ_H (ppm), mult. (*J* in Hz)	
	Renieramycin M (75 MHz)	**Renieramycin M** (Suwanborirux *et al.*, 2003) (125 MHz)	**Renieramycin M** (300 MHz)	**Renieramycin M** (Suwanborirux *et al.*, 2003) (500 MHz)
N-CH_3	41.5	41.5	2.26 (3H, s)	2.28 (3H, s)
CN	116.7	116.9	-	-
24	166.3	166.5	-	-
25	126.1	126.3	-	-
26	140.4	140.5	5.94 (1H, qq, 7.2, 1.1)	5.96 (1H, qq, 7.3, 1.5)
27	15.8	15.7	1.80 (3H, dq, 7.2, 1.2)	1.82 (3H, dq, 7.3, 1.5)
28	20.5	20.4	1.55 (3H, br s)	1.58 (3H, dq, 1.5, 1.2)

1.3.2.2 Renieramycin O

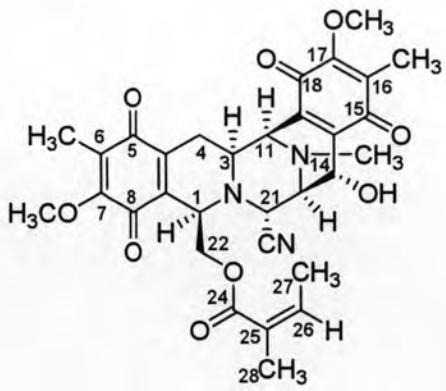

The ESI-TOF mass spectrum of renieramycin O showed a protonated molecular ion $[M+H]^+$ at *m/z* 592 implying a molecular formula of $C_{31}H_{33}N_3O_9$ (Figure 54). The molecular formula of renieramycin O revealed one more oxygen atom than renieramycin M.

The proton and carbon assignments of renieramycin O in the ^1H NMR spectrum (Figure 55) and the ^{13}C NMR spectrum (Figure 56) were achieved by comparison with the previous NMR data of renieramycin O (Suwanborirux *et al.*, 2003) as shown in Table 14. The ^1H and ^{13}C NMR spectra of renieramycin O were almost identical to those of renieramycin M. The methylene protons of C-14 (δ 2.73 ppm, 14-H α and 2.28 ppm, 14-Hβ) in the ^1H NMR spectrum and the methylene carbon of C-14 (δ 21.5 ppm) in the ^{13}C NMR spectrum of renieramycin M were not observed in those of renieramycin O. Interesting, a methine proton signal at δ 4.42 ppm (14-Hβ) and a hydroxyl proton (δ 3.75 ppm) were found. Moreover, the corresponding methine carbon signal at δ 62.2 ppm (C-14) was present in the ^{13}C NMR spectrum. This information implied the placement of a hydroxyl group at C-14 position. The coupling between the signals of 14-H and 13-H (δ 3.50 ppm) was absent. Therefore, the 14-H oriented β position, whereas 14-OH oriented α position.

Table 14 ^{1}H NMR and ^{13}C NMR assignments for renieramycin O in $CDCl_3$.

Position	δ_C (ppm)		δ_H (ppm), mult. (*J* in Hz)	
	Renieramycin O (75 MHz)	**Renieramycin O** (Suwanborirux *et al.*, 2003) (125 MHz)	**Renieramycin O** (300 MHz)	**Renieramycin O** (Suwanborirux *et al.*, 2003) (500 MHz)
1	56.1	56.4	4.00 (1H, overlap)	3.98 (1H, m)
3	53.2	53.4	3.10 (1H, d, 11.0)	3.05 (1H, ddd, 11.6, 3.3, 2.3)
4	25.3	25.3	α 2.86 (1H, d, 17.0) β 1.26 (1H)	α 2.87 (1H, dd, 17.2, 2.3) β 1.20 (1H,ddd, 17.2,11.6, 2.6)
5	185.0	185.4	-	-
6	128.7	128.6	-	-
7	155.7	155.6	-	-
8	180.5	180.8	-	-
9	135.5	135.7	-	-
10	140.7	141.1	-	-
11	55.2	55.0	4.06 (1H, br s)	4.09 (1H, dd, 3.3, 1.3)
13	62.5	62.4	3.50 (1H, br s)	3.42 (1H, br s)
14	62.2	62.0	α - β 4.42 (1H,s)	α - β 4.37 (1H, s)
15	187.1	187.8	-	-
16	128.2	128.4	-	-
17	155.3	155.8	-	-
18	182.2	182.8	-	-
19	135.5	135.3	-	-
20	141.0	141.0	-	-
21	56.4	56.4	4.27 (1H, br s)	4.23 (1H, d, 2.6)
22	62.2	62.1	a 4.49 (1H, d, 11.5) b 4.09 (1H, d, 11.5)	a 4.53 (1H, dd, 11.6, 3.0) b 4.09 (1H, dd, 11.6, 3.4)
6-CH_3	8.6	8.4	1.90 (3H, s)	1.92 (3H, s)
16-CH_3	8.9	8.7	1.90 (3H, s)	1.94 (3H, s)
7-OCH_3	61.1	61.1	4.00 (3H, s)	4.02 (3H, s)
17-OCH_3	61.1	61.1	4.01 (3H, s)	4.03 (3H, s)

Table 14 (continued).

Position	δ_C (ppm)		δ_H (ppm), mult. (*J* in Hz)	
	Renieramycin O (75 MHz)	**Renieramycin O** (Suwanborirux *et al.*, 2003) (125 MHz)	**Renieramycin O** (300 MHz)	**Renieramycin O** (Suwanborirux *et al.*, 2003) (500 MHz)
N-CH_3	42.5	42.4	2.50 (3H, s)	2.46 (3H, s)
14-OH	-	-	3.75 (1H, br s)	3.57 (1H, br s)
CN	116.1	116.3	-	-
24	166.4	166.5	-	-
25	126.1	126.2	-	-
26	140.4	140.6	5.95 (1H, q, 7.1)	5.98 (1H, qq, 7.3, 1.7)
27	15.8	15.7	1.79 (3H, d, 7.1)	1.82 (3H, dq, 7.3, 1.3)
28	20.4	20.3	1.54 (3H, br s)	1.57 (3H, dq, 1.7, 1.3)

1.3.2.3 Renieramycin N

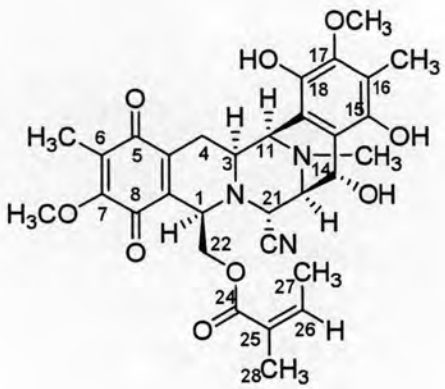

renieramycin N

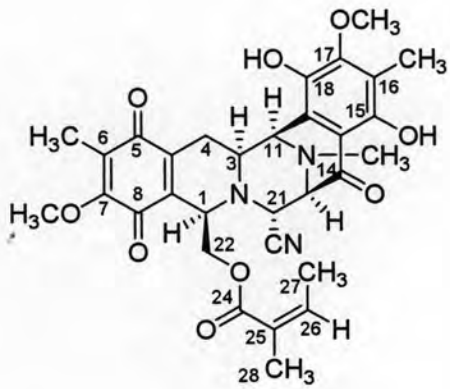

renieramycin Q

The ESI-TOF mass spectrum of renieramycin N showed a protonated molecular ion $[M+H]^+$ at *m/z* 594 implying a molecular formula of $C_{31}H_{35}N_3O_9$ (Figure 51). The molecular weight of renieramycin N was 18 mass units higher than that of renieramycin M. The proton and carbon assignments of renieramycin N were similar to renieramycin Q from the previous report except chemical shift of the carbon at C-14 (Amnouypol *et al.*, 2004) as shown in Table 15. In this presentation, we could not compare chemical shift of protons and carbons of renieramycin N with the previous data which were recorded in pyridine. The 300 MHz ^1H and 75 MHz ^{13}C NMR spectra of renieramycin N in $CDCl_3$ (Figures 52 and 53) revealed the methine proton signal of 14-H appearing as a board singlet at δ 4.55 ppm and the corresponding methine carbon signal also shifted upfield to δ 64.1 (C-14) as compared to renieramycin Q (δ 198.4 ppm) (Amnouypol *et al.*, 2004). This indicated the presence of the 14α-hydroxy substitution of renieramycin N. Moreover, the ^{13}C NMR of renieramycin N, which was different from those bisquinone renieramycins, showed only two quinone carbon signals at 180.8 ppm (C-8) and 185.6 ppm (C-5). These data implied that one of the quinone rings in renieramycin N has been reduced to a hydroquinone ring. In addition, a pair of the phenolic carbon signals at δ 146.2 and 139.0 ppm for renieramycin N also supported the presence of the hydroquinone ring.

Table 15 ^{1}H NMR and ^{13}C NMR assignments for renieramycin N and renieramycin Q in $CDCl_3$.

Position	δ_C (ppm)		δ_H (ppm), mult. (*J* in Hz)		
	Renieramycin N (75 MHz)	**Renieramycin Q** (Amnuoypol *et al.*, 2004) (125 MHz)	**Renieramycin N** (300 MHz)	**Renieramycin Q** (300 MHz)	**Renieramycin Q** (Amnuoypol *et al.*, 2004) (500 MHz)
1	56.1	54.8	3.95 (1H,br s)	4.08 (1H, br s)	3.95 (1H, dt, 3.4, 2.5)
3	54.4	53.8	3.08 (1H, br d, 2.6)	3.44 (1H, d, 11.5)	3.23 (1H, ddd, 11.0, 3.1, 2.5)
4	24.6	24.1	α 3.03 (1H) β 1.30 (1H)	α 3.10 (1H, d, 17.3) β 1.60 (1H, ddd, 17.3, 11.5, 2.8)	α 3.03 (1H, dd, 17.7, 2.5) β 1.54 (1H,ddd, 17.7,11.0, 2.5)
5	185.6	185.7	-	-	-
6	128.3	128.0	-	-	-
7	155.6	156.0	-	-	-
8	180.8	180.7	-	-	-
9	135.2	135.6	-	-	-
10	142.2	141.4	-	-	-
11	56.7	56.5	4.01 (1H, br s)	4.42 (1H, br s)	4.28 (1H, dd, 3.3, 0.5)
13	64.2	66.2	3.44 (1H, br s)	3.61 (1H, br s)	3.37 (1H, dd, 1.0, 0.5)
14	64.1	198.4	α - β 4.55 (1H, br s)	-	-
15	146.2	155.0	-	-	-
16	118.9	118.4	-	-	-
17	144.9	153.0	-	-	-
18	139.0	139.3	-	-	-
19	118.0	117.7	-	-	-
20	114.5	112.2	-	-	-
21	56.5	56.0	4.58 (1H, d, 2.8)	4.51 (1H, br s)	4.31 (1H, d, 1.0)
22	61.6	62.0	a 4.22 (1H, dd, 11.0, 2.3) b 4.00 (1H, d, 11.0)	a 4.08 (1H, overlap) b 4.04 (1H, overlap)	a 4.09 (1H, dd, 11.6, 3.4) b 4.02 (1H, dd, 11.6, 2.5)

Table 15 (continued).

Position	δ_C (ppm)		δ_H (ppm), mult. (*J* in Hz)		
	Renieramycin N (75 MHz)	**Renieramycin Q** (Amnuoypol *et al.*, 2004) (125 MHz)	**Renieramycin N** (300 MHz)	**Renieramycin Q** (300 MHz)	**Renieramycin Q** (Amnuoypol *et al.*, 2004) (500 MHz)
6-CH_3	8.9	8.6	1.91 (3H, s)	1.90 (3H, s)	1.85 (3H, s)
16-CH_3	9.3	8.8	2.13 (3H, s)	2.14 (3H, s)	2.09 (3H, s)
7-OCH_3	61.1	61.1	3.98 (3H, s)	4.00 (3H, s)	3.94 (3H, s)
17-OCH_3	61.0	61.0	3.73 (3H, s)	3.86 (3H, s)	3.79 (3H, s)
N-CH_3	42.9	42.4	2.46 (3H, s)	2.55 (3H, s)	2.38 (3H, s)
14-OH	-	-	-	-	-
15-OH	-	-	-	11.38 (1H, s)	11.40 (1H, s)
18-OH	-	-	-	-	5.51 (1H, s)
CN	116.7	115.9	-	-	-
24	166.9	166.6	-	-	-
25	126.5	126.5	-	-	-
26	140.0	139.6	5.84 (1H, qq, 7.2, 1.2)	5.88 (1H, q, 7.3)	5.81 (1H, qq, 7.3, 1.3)
27	15.7	15.4	1.75 (3H, dq, 7.2, 1.1)	1.78 (3H, d, 7.3)	1.68 (3H, dq, 7.3, 1.6)
28	20.0	19.8	1.59 (3H, br s)	1.60 (3H)	1.54 (3H, dq, 1.6, 1.3)

1.3.2.4 Renieramycin Q

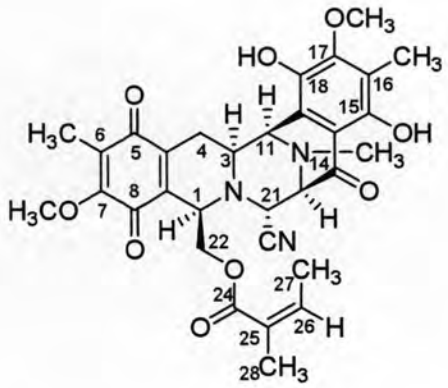

The ESI-TOF mass spectrum of renieramycin Q showed a protonated molecular ion $[M+H]^+$ at *m/z* 592 implying a molecular formula of $C_{31}H_{33}N_3O_9$ (Figure 57). The molecular weight of renieramycin Q was 2 mass units lower than that of renieramycin N. The 300 MHz ^1H NMR spectrum (Figure 58) of renieramycin Q showed similarity to previously reported proton NMR data of renieramycin Q (Amnouypol *et al.*, 2004) as shown above in Table 15. These data confirmed that this compound was renieramycin Q.

1.3.2.5 Mimosamycin

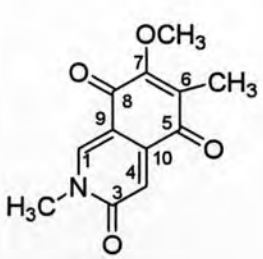

Mimosamycin is a simple isoquinoline alkaloid. It was obtained as a yellow amorphous solid. This compound has the molecular formula $C_{12}H_{11}NO_4$ as deduced by ESI-TOF MS (Figure 59), showing a protonated molecular ion peak of $[M+H]^+$ at *m/z* 234. Mimosamycin was assigned the structure by analysis of the NMR spectra and comparison reported data (Saito *et al.*, 2004). The 300 MHz ^1H NMR spectrum (Figure 60) revealed the signals of two singlet olefinic protons at δ 8.24 ppm (H-1)

and 7.09 ppm (H-4). Three remaining singlet signals were the signals of 7-OCH_3 (δ 4.15 ppm), 2-NCH_3 (δ 3.64 ppm), and 6-CH_3 (δ 2.04 ppm). The 75 MHz ^{13}C NMR spectrum (Figure 61) showed the signals of three carbonyl carbons at δ 183.2, 177.1, and 162.6 ppm. These carbons were assigned as C-5, C-8, and C-3, respectively. The four quarternary sp^2 carbons were C-6 (δ 133.6 ppm), C-7 (δ 159.3 ppm), C-9 (111.2 ppm), and C-10 (138.7 ppm). The downfield methyl signals at δ 61.3 and 38.5 ppm were assigned as 7-OCH_3 and 2-NCH_3. The aryl methyl 6-CH_3 appeared at δ 9.7 ppm. The assignments are summarized in Table 16.

Table 16 ^{1}H NMR and ^{13}C NMR assignments for mimosamycin in $CDCl_3$.

Position	δ_H (ppm), mult. (*J* in Hz)		δ_C (ppm)	
	Mimosamycin 300 MHz	**Mimosamycin** (Saito *et al.*, 2004) 270 MHz	**Mimosamycin** 75 MHz	**Mimosamycin** (Saito *et al.*, 2004) 67.5 MHz
1	8.24	8.27	141.9	142.1
3	-	-	162.6	162.8
4	7.09	7.10	116.6	116.7
5	-	-	183.2	183.5
6	-	-	133.0	133.1
7	-	-	159.3	159.5
8	-	-	177.1	177.3
9	-	-	111.2	111.3
10	-	-	138.7	138.9
7-OCH_3	4.15	4.17	61.3	61.3
6-CH_3	2.04	2.06	9.7	9.5
2-NCH_3	3.64	3.67	38.5	38.4

1.4 Cytotoxicity of jorunnamycins A-C

The cytotoxicity against three tumor cell lines of jorunnamycins A-C including human colon carcinoma (HCT116), human lung carcinoma (QG56), and human prostate carcinoma (DU145) is summarized in Table 17. Jorunnamycin C displayed nanomolar inhibitory effect that is almost the same as those of jorumycin and ecteinascidin 770. Jorunnamycin A exhibited much higher potency than jorunnamycin B but lower than jorumycin and renieramycin M. This information supports that the oxygenation at C-14 dramatically diminishes cytotoxicity and the

ester side chain at C-22 is required for potent cytotoxicity of the marine bistetrahydroisoquinolines.

Table 17 Cytotoxicity of jorunnamycins A-C to various cancer cell lines (IC_{50} nM)[a].

Compound	HCT116	QG56	DU145
Jorunnamycin A	13	59	29
Jorunnamycin B	455	618	448
Jorunnamycin C	1.5	2.8	0.32
Renieramycin M	7.9	19	NT
Jorumycin	0.57	0.76	0.49
Ecteinascidin 770	0.40	1.8	0.66

[a] HCT116 = human colon carcinoma; QG56 = human lung carcinoma; DU145 = human prostate carcinoma.
NT = not tested.

2. Structure modification of renieramycin M

Although renieramycins have been discovered from marine organisms for over 25 years and showed potent cytotoxic activity comparable to the related saframycins, there have been a few investigations for their chemical and biological properties. Due to the α-carbinolamine function causing the degradation of renieramycins during the conventional extraction process, the availability of the compounds from natural sources has been so limited. Suwanborirux and co-workers have succeeded in large-scale preparation of the stabilized renieramycin M from the Thai blue sponge, *Xestospongia* sp. by pretreatment the sponge with potassium cyanide before extraction process (Suwanborirux *et al.*, 2003). Since renieramycin M was available in high yield from the abundant sponge *Xestospongia* sp., the author has been interested in preparing renieramycin analogs which might have higher activity and could be used to study the mechanism of action. After the isolation of jorumycin from the nudibranch, *Jorunna funebris*, the preliminary results for jorumycin indicated remarkable cytotoxicity against NIH 3T3 fibroblast cells and some tumor cell lines, such as P388 mouse lymphoma, A549 human lung carcinoma, HT29 human colon carcinoma, and MEL28 human melanoma, at very low concentrations (Fontana *et al.*, 2000). The structure of jorumycin is related to renieramycin E except the presence of an acetyl ester at C-22 in jorumycin instead of an angelate ester in renieramycin E. Moreover, Myer and Plowright reported the synthesis of a series of saframycin A acyl analogs from the pentacycle intermediat, **81** via the removal of the

Fmoc group followed by coupling of several acids to the primary amine at C-22 (Scheme 8). All of the acyl derivatives showed potent activity against A 375 melanoma and A549 lung carcinoma tumor cell lines as shown in Table 3 (Mayer and Plowright, 2001).

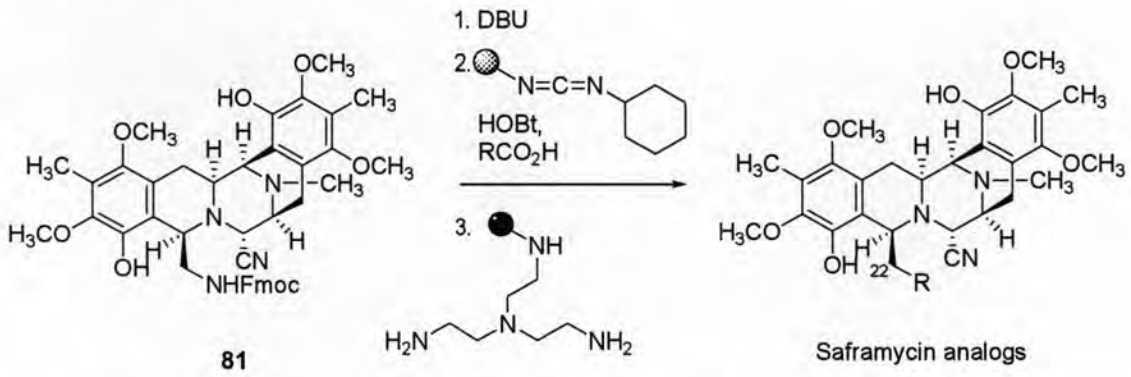

Scheme 8 Synthesis of saframycin A analogs.

The saframycin analog QAD (**21**) is a quinaldic acyl derivative of saframycin A. It also showed high cytotoxicity (Spencer *et al.*, 2006). Other bistetrahydroisoquinoline containing a phthalamide at C-22, phthalascidin (Pt 650), an analog of ecteinascidin 743, was successfully synthesized based on the synthetic route of ecteinascidin 743 (*Martinez et al.*, 2000). It showed indistinguishable cytotoxicity from ecteinascidin 743. The above information suggested the importance of the acyl group for potent cytotoxicity. In this thesis, the acylation at C-22 of renieramycin M to several acyclic, alicyclic, and aromatic ester derivatives are prepared from the key intermediate deangeloylrenieramycin M and cytotoxicity evaluation is also conducted.

2.1 Transformation of renieramycin M to deangeloylrenieramycin M

The intermediate deangeloylrenieramycin M in 43.4% yield was prepared by two step transformations of renieramycin M via the leuco compound, renieramycin M bisdihydroquinonerenieramycin M (Saito *et al.*, 2004). According to our previous procedure, the preparation of deangeloylrenieramycin M was first succeeded by catalytic hydrogenation over 20% $Pd(OH)_2/C$ and immediately subsequent reduction with AlH_3 in THF and air oxidation. This reaction also yielded the recovered renieramycin M (10.0%) as shown in Scheme 9. Comparison ^1H NMR (Figures 11 and 49) and ^{13}C NMR (Figures 13 and 50) spectral data between

deangeloylrenieramycin M and renieramycin M revealed that deangeloylrenieramycin M showed signals almost identical to those of renieramycin M except the angelate signals [δ_H 5.96/δ_C 140.5 (H-26), δ_H 1.82/δ_C 15.7 (CH_3-27), δ_H 1.58/δ_C 20.4 (CH_3-28), δ_C 166.5 (C-24), and δ_C 126.3 (C-25)]. In addition, the methylene proton signals at C-22 of deangeloylrenieramycin M shifted upfield to δ_H 3.48 and 3.71 ppm when compared with those of renieramycin M (δ_H 4.10 and 4.53 ppm) (Suwanborirux *et al.*, 2003).

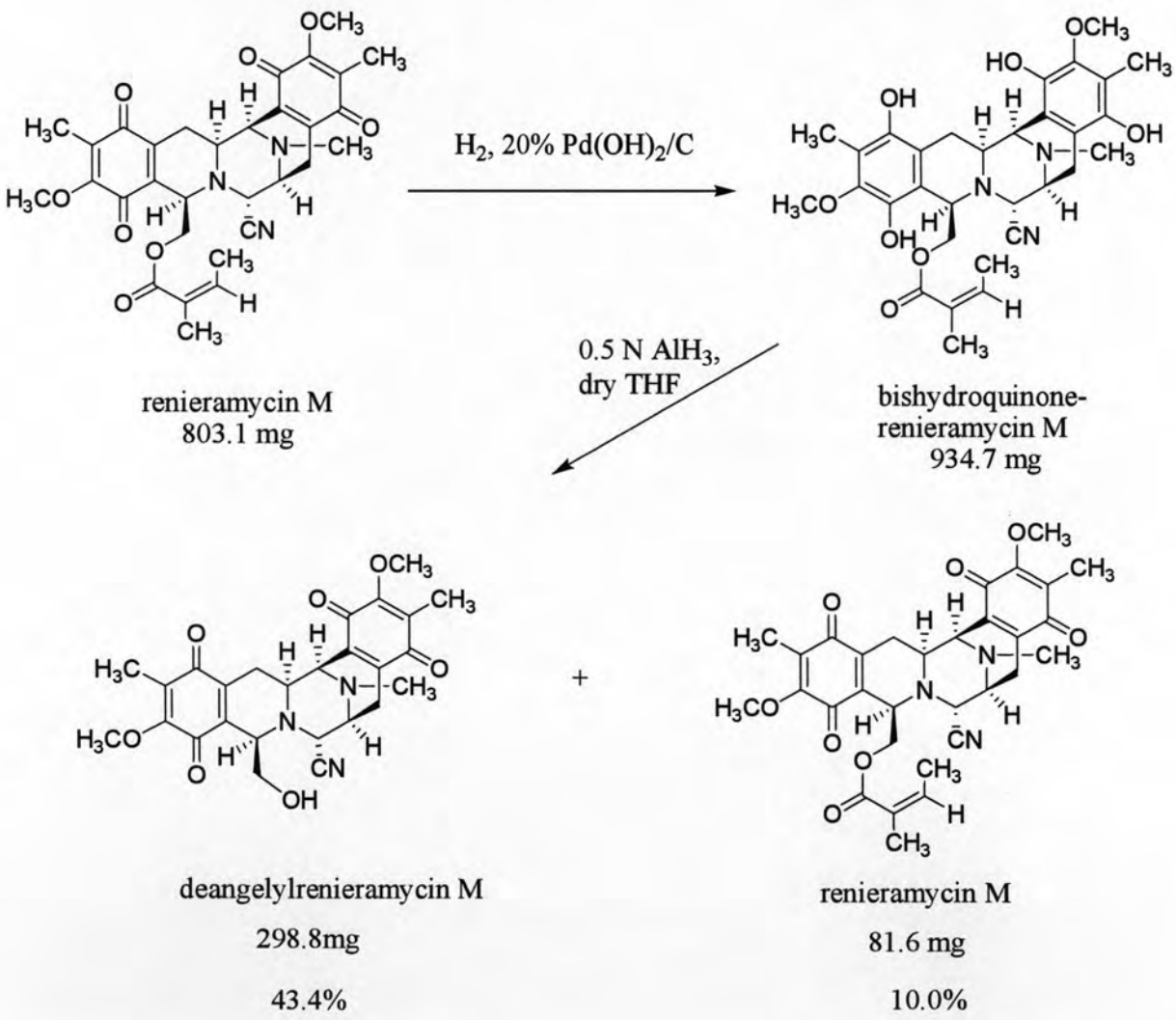

Scheme 9 Transformation of renieramycin M to deangeloylrenieramycin M.

2.2 Transformations of deangeloylrenieramycin M to 22-*O*-acyl renieramycin analogs

A series of 22-*O*-acyl renieramycin analogs were synthesized based on high cytotoxicity data of jorumycin containing and acetyl ester at C-22, saframycin analogs which varied aromatics amide bond forming at C-22, and phthalascidin (Pt 650). Moreover, renieramycin M possessed potent cytotoxicity than jorunnamycin A. This information suggests that the acyl side chain is required for the cytotoxicity. Acylations of deangeloylrenieramycin M into twenty-one renieramycin analogs including seven saturated acyclic acyl **60-66**, two unsaturated acyclic acyl **67** and **79**, three saturated alicyclic acyl **68-69** and **80**, four unsaturated alicyclic acyl **70-73**, and five aromatic acyl **74-78** renieramycin analogs were performed in 25-85% yields by treatment with the corresponding acid anhydrides or acid chlorides in the presence of pyridine as a solvent and 4-dimethylaminopyridine (DMAP) as a catalyst as shown in Table 18. The acyl parts at C-22 of acyclic renieramycin analogs vary in chain length from 1 carbon to 7 carbons as straight chains and branch chains. The acyl parts at C-22 of alicyclic and aromatic renieramycin analog were shown in the Table 18.

All analogs were prepared from corresponding acid anhydrides or acid chlorides. Acid anhydride was selected for the first choice in chemical reaction and acid chloride was chosen for the second choice because acid chloride is a strong reagent Analogs **62-63** and **65-66** were prepared from commercially available acid anhydrides.

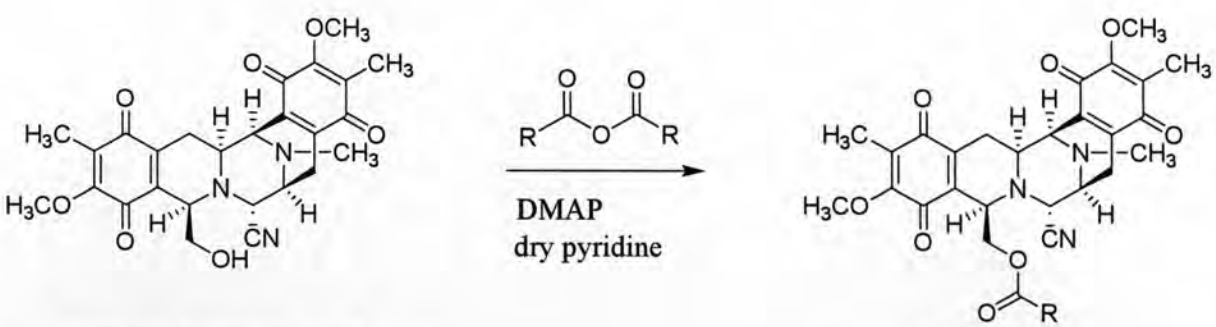

deangeloylrenieramycin M

62-63 and **65-66**

The acid anhydrides for preparation of analogs **67**, **71** and **73** were obtained by treatment of commercially available carboxylic acids with isopropyl chloroformate and anhydrous potassium carbonate (K_2CO_3). Analog **73** was obtained as a mixture

of diastereoisomers since the corresponding acid anhydride used was an enantiomeric mixture.

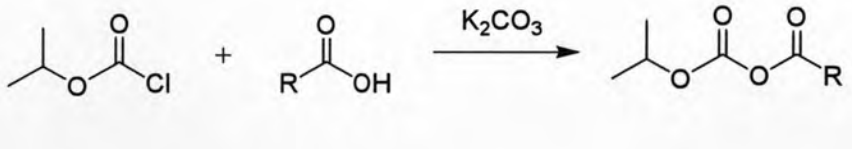

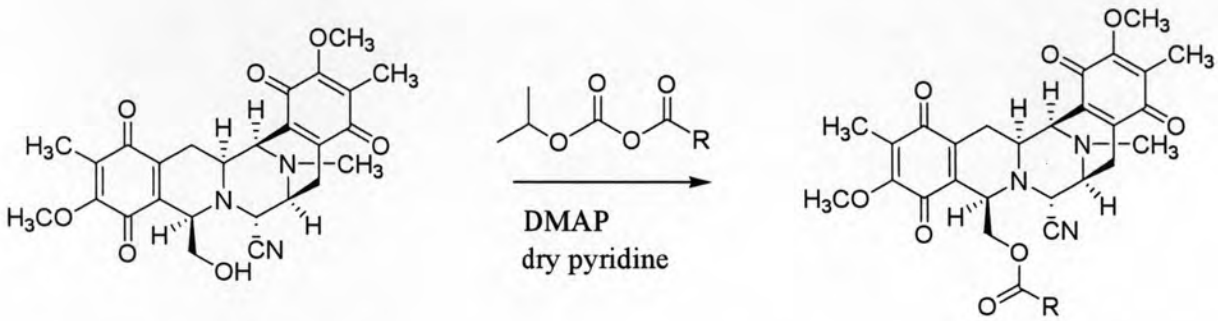

deangeloylrenieramycin M

67, 71, and **73**

The acetic formic anhydride for preparation of analog **60** was prepared from the reaction of acetyl chloride with sodium formate.

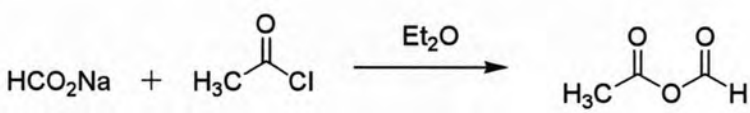

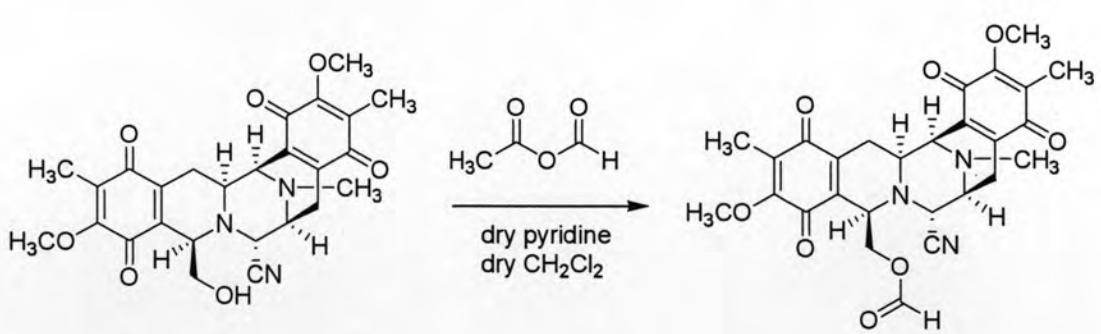

deangeloylrenieramycin M

60

The cyclohexanoic anhydride for preparation of analog **69** was prepared from the reaction of cyclohexanecarbonyl chloride with cyclohexanecarboxylic acid.

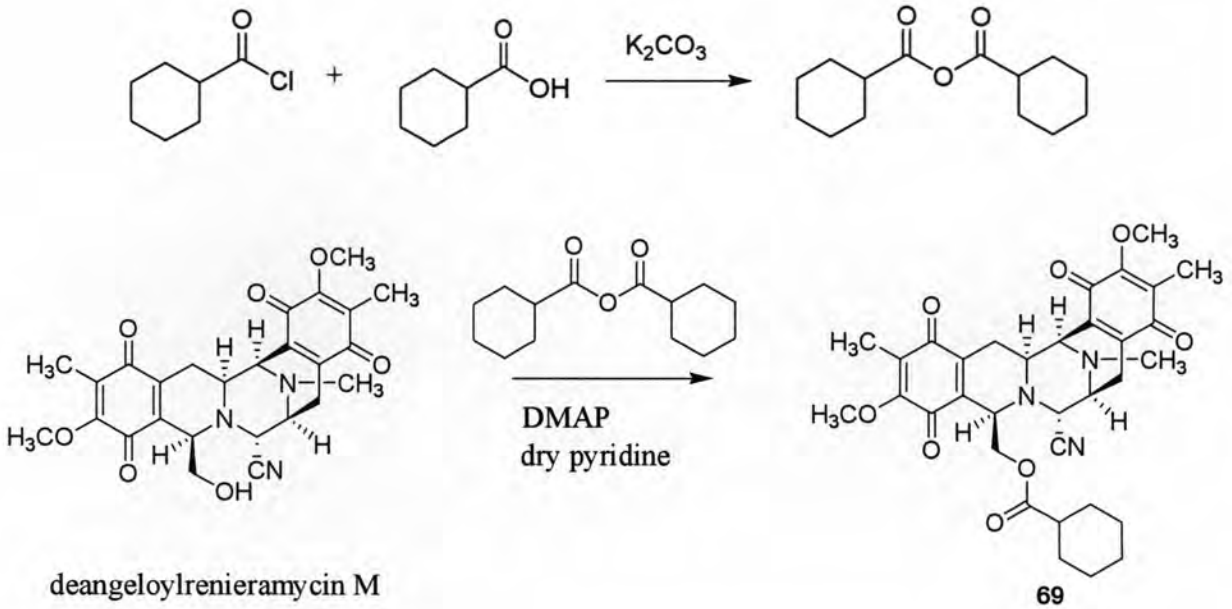

deangeloylrenieramycin M

69

Analogs **61**, **64**, **68**, and **74-77** were obtained from commercially available acid chlorides. Analog **64** was obtained as a mixture of diastereoisomers since the corresponding acid chloride used was an enantiomeric mixture. Acid chlorides for preparations of analogs **70**, **72**, and **78** were started from conversion of commercial carboxylic acids to carbonyl chlorides by using thionyl chloride.

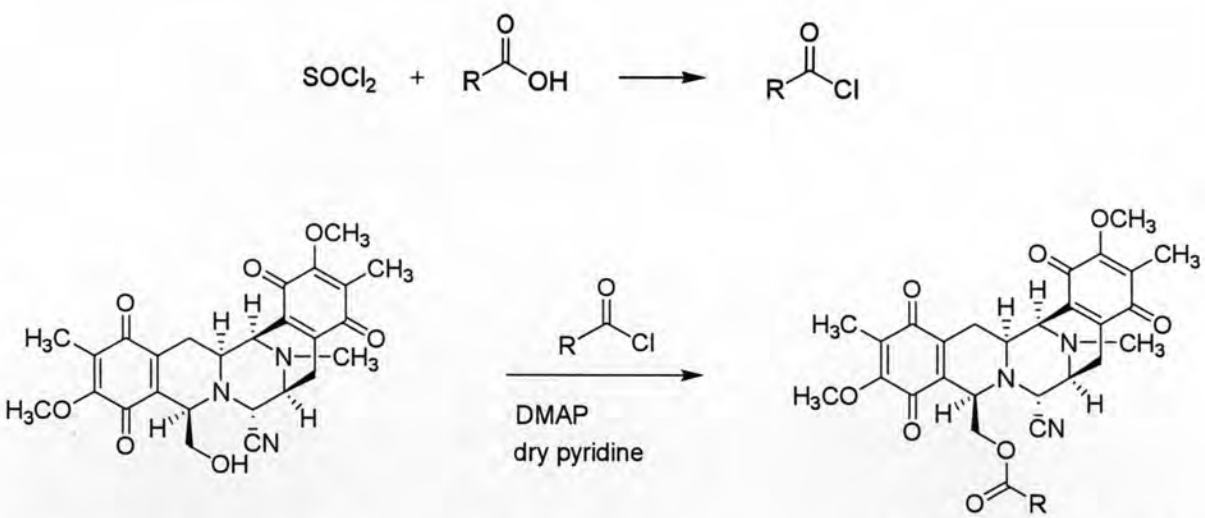

deangeloylrenieramycin M

61, 64, 68, 70, 72 and **74-78**

Conversions of 21-CN of **67** and **69** into 21-OH of **79** and **80** in 96% yield, respectively were easily achieved by treatment with silver nitrate in aqueous acetonitrile. The structures of renieramycin analogs were interpreted by using NMR

and MS data. Assignments for all protons and carbons were accomplished by analysing with 1D-NMR and 2D-NMR including DEPT, ^{1}H-^{1}H COSY, HMQC, HMBC, and NOESY.

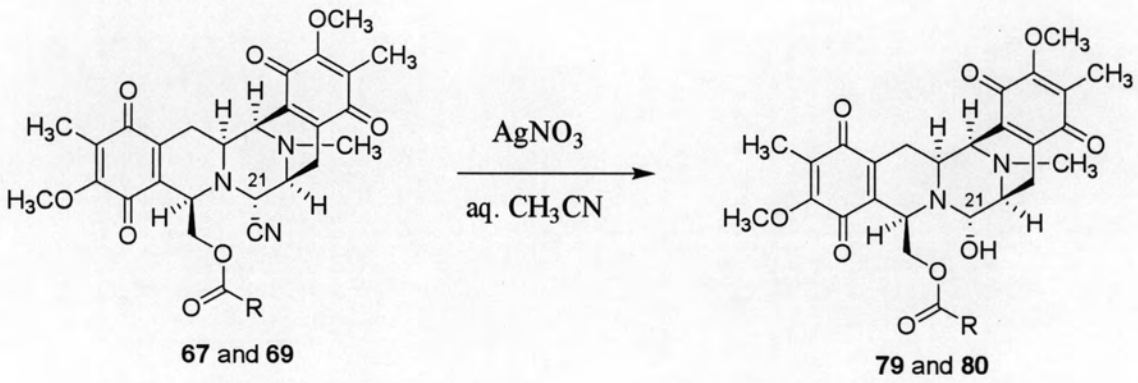

67 and **69** **79** and **80**

Table 18 Summary of % yields and high-resolution mass data of the 22-*O*-acyl renieramycin analogs.

Analog	R	% yields	Molecular formula	M.W. from HR-MS
60	H	45.2	$C_{27}H_{27}N_3O_8$	521.1792 (obsd.) 521.1798 (calcd.)
61		29.8	$C_{29}H_{30}ClN_3O_8$	583.1728 (obsd.) 583.1722 (calcd.)
62	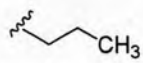	64.8	$C_{30}H_{33}N_3O_8$	563.2271 (obsd.) 563.2268 (calcd.)
63	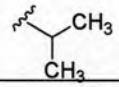	44.1	$C_{30}H_{33}N_3O_8$	563.2273 (obsd.) 563.2268 (calcd.)
64	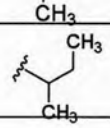	40.1	$C_{31}H_{35}N_3O_8$	577.2424 (obsd.) 577.2424 (calcd.)
65	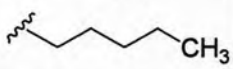	58.4	$C_{32}H_{37}N_3O_8$	591.2578 (obsd.) 591.2581 (calcd.)
66	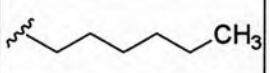	68.5	$C_{33}H_{39}N_3O_8$	605.2733 (obsd.) 605.2737 (calcd.)
67	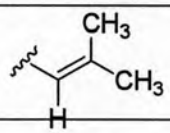	74.6	$C_{31}H_{33}N_3O_8$	575.2268 (obsd.) 575.2268 (calcd.)
68	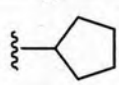	78.8	$C_{32}H_{35}N_3O_8$	589.2427 (obsd.) 589.2424 (calcd.)
69	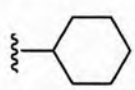	80.1	$C_{33}H_{37}N_3O_8$	603.2584 (obsd.) 603.2581 (calcd.)
70	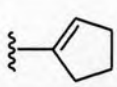	60.5	$C_{32}H_{33}N_3O_8$	587.2267 (obsd.) 587.2268 (calcd.)
71	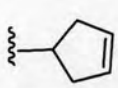	64.4	$C_{32}H_{33}N_3O_8$	587.2267 (obsd.) 587.2268 (calcd.)
72	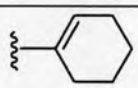	58.4	$C_{33}H_{35}N_3O_8$	601.2427 (obsd.) 601.2424 (calcd.)

Table 18 (continued).

Analog	R	% yields	Molecular formula	M.W. from HR-MS
73	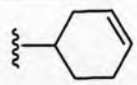	80.4	$C_{33}H_{35}N_3O_8$	601.2420 (obsd.) 601.2424 (calcd.)
74	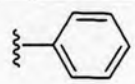	39.4	$C_{33}H_{31}N_3O_8$	597.2115 (obsd.) 597.2111 (calcd.)
75	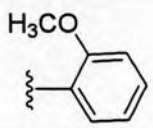	54.9	$C_{34}H_{33}N_3O_9$	628.2298 $[M+H]^+$ (obsd.) 628.2295 $[M+H]^+$ (calcd.)
76	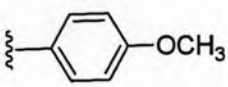	44.0	$C_{34}H_{33}N_3O_9$	627.2220 (obsd.) 627.2217 (calcd.)
77	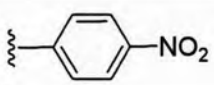	48.6	$C_{33}H_{30}N_4O_{10}$	643.2037 $[M+H]^+$ (obsd.) 643.2030 $[M+H]^+$ (calcd.)
78	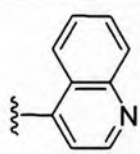	67.1	$C_{36}H_{32}N_4O_8$	649.2296 $[M+H]^+$ (obsd.) 649.2299 $[M+H]^+$ (calcd.)
79	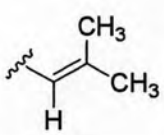	97.0	$C_{30}H_{34}N_2O_9$	549.2241 $[M+H-H_2O]^+$ (obsd.) 549.2237 $[M+H-H_2O]^+$ (calcd.)
80	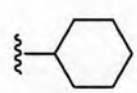	95.6	$C_{32}H_{38}N_2O_9$	577.2553 $[M+H-H_2O]^+$ (obsd) 577.2550 $[M+H-H_2O]^+$ (calcd.)

2.2.1 22-*O*- acyclic acyl renieramycin analogs

The HR-MS data of 22-*O*- acyclic acyl renieramycin analogs **60-67** and **79** were shown in Table 18. The HR mass spectral data of these analogs except **65** and **79** showed the same major fragment ion at *m/z* 220 $[C_{12}H_{14}NO_3]^+$ as shown in Scheme 10.

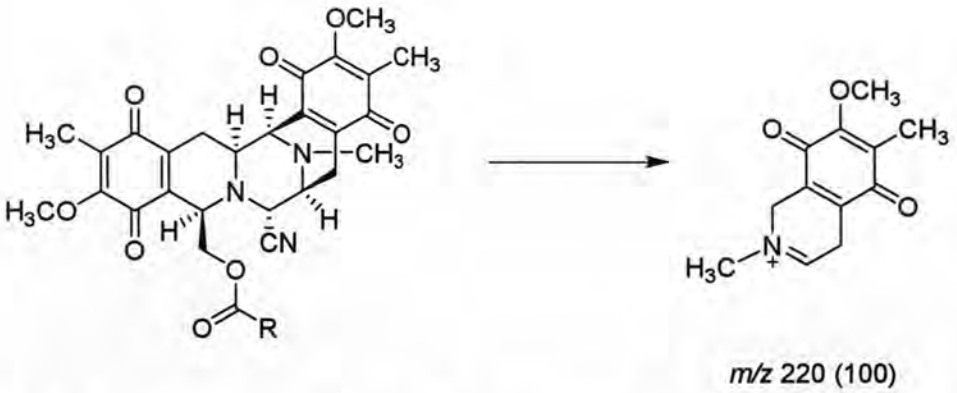

Scheme 10 Fragment ion at *m/z* 220 of some acyclic acyl renieramycin analogs.

The HR-FABMS of analog **79** did not reveal a protonated molecular ion $[M+H]^+$ peak at *m/z* 567 but presented $[M+H-H_2O]^+$ peak at *m/z* 549 corresponding to tentative molecular formula $C_{30}H_{34}N_2O_9$. The 9 mass unit difference from analog **67** suggested that the replacement of the cyano group in analog **67** by the hydroxyl group. Moreover, the IR spectrum of analog **79** showed the absence of absorption band for cyanide and the presence of hydroxyl absorption at 3468 cm^{-1}. The IR spectra of these analogs revealed characteristic absorption bands for ester carbonyl at 1710-1740 cm^{-1}, cyanide (CN) at 2228 cm^{-1} and quinone carbonyl at 1615, 1650 cm^{-1} implying the quinone characters. The UV spectra exhibited λ_{max} at 267-270 nm and the optical rotations showed negative value about -95 to -60.

The protons and carbons assignments were performed by 1D-NMR and 2D-NMR, including ^1H-^1H COSY, HMQC, HMBC, and NOESY and compared with NMR data of deangeloylrenieramycin M. In general, the 500 MHz ^1H NMR and 125 MHz ^{13}C NMR spectra in $CDCl_3$ of all acyclic acyl renieramycin analogs showed signals similar to those of deangeloylrenieramycin M as shown in Table 10. The 500 MHz ^1H NMR spectrum of acyclic acyl renieramycin derivatives contained two aryl methyl proton groups at $\delta \sim 1.80$-1.98 ppm while the aryl methoxyl protons at $\delta \sim$ 3.90-4.03 ppm and the *N*-methyl signal at $\delta \sim 2.20$-2.30 ppm. The characteristic 4-Hβ signal appeared as a doublet of doublets of doublets resulting from the geminal coupling with 4-Hα ($J \sim 17$-18 Hz), the vicinal coupling with 3-H ($J \sim 11$ Hz), and the unique homoallylic coupling with 1-H ($J \sim 2$-3 Hz). Interestingly, the methylene proton signals at C-22 of acyclic acyl renieramycin analogs shifted downfield to δ_H 3.90-4.10 and 4.10-4.60 ppm when compared with those of deangeloylrenieramycin M δ_H 3.48 and 3.71 ppm. Acyclic acyl side chains at C-22 of derivatives **60-66**,

almost showed the signals of methylene protons at ~ 2.50-1.00 ppm; methyl protons at ~ 0.80-1.00 ppm. The methylene protons which connected to chlorine atom of analog **61** showed downfield chemical shift at 3.53 ppm. Analogs **63** and **64** additionally showed a group of methine proton at δ 2.30 ppm and 2.02 ppm, respectively. Analog **60** displayed a very downfield aldehyde proton at 7.80 ppm. Other analogs **67** and **79** revealed signals for olefinic protons at ~5.20 ppm as shown in Table 19.

The 125 MHz ^{13}C NMR spectra of all acyclic acyl derivatives revealed quinone carbonyl carbons and ester carbons signal at δ ~ 180-187 ppm and at δ ~ 160-175 ppm, respectively. The signals of the cyano carbons appeared at δ ~ 116-117 ppm (21-CN) and C-21 at ~ 58-59 ppm. However, C-21 of analog **79** shifted downfield to δ 82.8 ppm comparable to that of the analog **67** at δ 58.8 ppm. Two methoxy carbons appeared at δ ~ 60-61 ppm (7 and 17-OCH_3). *N*-methyl carbons showed at ~ 41-42 ppm. Two methyl carbons of quinone rings revealed at ~ 8-9 ppm (6, 16-CH_3). Analog **79** showed different chemical shift for carbons at C-1, C-3 and C-13 from deangeloylrenieramycin M. C-1 and C-3 of derivative **79** shifted upfield to 53.0 and 51.0 ppm, respectively (Figure 173). C-13 of analog **79** shifted downfield to 57.6 ppm (Figure 173). Acyclic acyl side chains at C-22 of derivatives **60-66**, mostly showed the signals of methine carbons at ~ 35-41 ppm; methylene carbons at ~ 20-38 ppm; methyl carbons at ~ 10-20 ppm. Analogs **67** and **79** exhibited two olefinic carbons at ~ 114-116 ppm (C-2') and at ~ 114 -116 ppm (C-3') as shown in Table 19. Analog **64** was obtained as a mixture of unseparable diastereoisomers since the corresponding acid chloride used was an enantiomeric mixture. The ^{1}H NMR of analog **64** clearly showed pairs signals of 22-Ha at δ 4.17 ppm (major isomer) and 4.20 ppm (minor isomer); 22-Hb at δ 4.05 ppm (minor and major isomer). In addition, the ^{13}C NMR of analog **64** also showed pairs signals of C-5 at δ 185.41 ppm (major isomer) and 185.43 ppm (minor isomer); C-15 at δ 186.22 ppm (major isomer) and 186.24 ppm (minor isomer). The ratio of major and minor isomer was 3 : 2.

Table 19 ^{1}H NMR and ^{13}C NMR spectral data of the acyl part of the 22-*O*-acyl renieramycin analogs.

Analog	Substitute (R)	NMR assignments	
		δ_H (*J* in Hz)	δ_C
60	H	7.80 (1H, s)	159.8 (OCO)
61	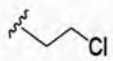	3.53 (2H, m,), 2.53 (2H, m)	38.5, 37.4, 169.5 (OCO)
62	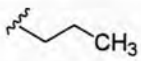	2.01 (2H, t, 7.3), 1.42 (2H, sept, 7.3), 0.82 (3H, t, 7.3)	36.0, 18.3, 13.6, 172.6 (OCO)
63	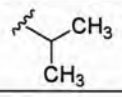	2.30 (1H, overlap), 0.95 (3H, d, 7.0), 0.93 (3H, d, 10.1)	33.8, 19.0, 18.5, 176.0 (OCO)
64	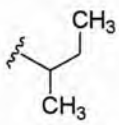	Minor: 2.02 (1H, m), 1.20 (2H), 0.84 (3H, d, 7.0), 0.67 (3H, td, 7.6, 1.5) Major: 2.02 (1H, m), 1.23 (2H), 0.82 (3H, d, 7.0), 0.81 (3H, td, 7.2, 1.2)	Minor: 40.8, 26.2, 15.9, 11.4, 175.7 (OCO) Major: 40.8, 26.6, 16.5, 14.1, 175.7 (OCO)
65	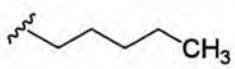	2.02 (2H, t, 8.3), 1.40 (2H, sextet, 8.3), 1.23 (2H, m), 1.16 (2H, m), 0.85 (3H, t, 7.3)	34.0, 31.2, 24.4, 22.3, 13.8, 172.8 (OCO)
66	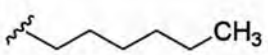	1.95 (2H, t, 8.9), 1.32 (2H, m), 1.19 (2H, m), 1.12 (2H, m), 1.11 (2H, m), 0.80 (3H, t, 7.2)	34.1, 31.1, 28.7, 24.7, 22.4, 13.9, 172.8 (OCO)
67	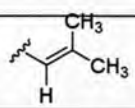	5.23 (1H, br s), 1.94 (3H, s), 1.74 (3H, s)	158.7, 114.8, 27.4, 20.2, 165.4 (OCO)
68	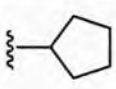	2.36 (1H, quintet, 7.5), 1.59 (2H, m), 1.58 (2H, m), 1.45 (1H, m),1.43 (2H, m), 1.39 (1H, m)	43.8, 30.1, 29.7, 25.6, 25.5, 175.7 (OCO)
69	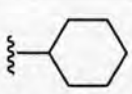	1.91 (1H, overlap), 1.56 (2H, m), 1.55 (2H, m), 1.52 (2H, m), 1.06 (2H, m), 1.04 (2H, m),	43.0, 29.3, 28.7, 25.5 (2C), 25.4, 175.0 (OCO)
70	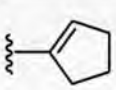	6.38 (1H, dt, 6.4, 2.1), 2.31 (2H, m), 2.20 (2H, overlap), 1.77 (2H, quintet, 7.6)	144.7, 134.8, 33.3, 31.2, 22.9, 164.1 (OCO)
71	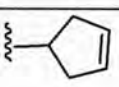	5.46 (2H, m), 2.77 (2H, t, 7.0), 2.77 (1H, quintet, 7.0), 2.34 (2H, m)	129.1, 128.6, 41.6, 36.3, 35.7, 175.0 (OCO)

Table 19 (continued).

Analog	Substitute (R)	NMR assignments	
		δ_H (*J* in Hz)	δ_C
72	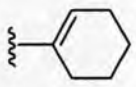	6.58 (1H, m), 1.99 (2H, m), 1.88 (2H, overlap), 1.87 (2H, overlap), 1.44 (2H, m)	140.6, 129.6, 25.7, 24.0, 21.9, 21.2, 166.5 (OCO)
73	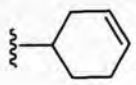	Minor: 5.53 (1H, m), 5.44 (1H, m), 2.19 (1H, m), 197 (1H, m), 1.94 (1H, m), 1.87 (1H, m), 1.80 (1H, m), 1.28 (2H, m) Major: 5.71 (2H, m), 2.19 (1H, m), 1.97 (1H, m), 1.94 (1H, m), 1.87(1H, m), 1.80 (1H, m), 1.28 (2H, m)	Minor: 126.6, 124.6, 39.1, 27.7, 25.2, 24.3, 174.8 (OCO) Major: 126.9, 124.8, 39.2, 27.7, 25.5, 24.3, 174.8 (OCO)
74	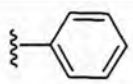	7.60 (2H, dd, 7.7, 1.2), 7.50 (1H, dt, 7.7, 1.6), 7.31 (2H, t, 7.7)	133.1, 130.0, 129.2 (2C), 128.4 (2C), 165.2 (OCO)
75	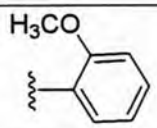	7.50 (1H, dd, 7.7, 1.6), 7.41 (1H, dt, 7.7, 1.6), 6.88 (1H, t, 7.7), 6.85 (1H, d, 7.7)	158.5, 133.9, 132.3, 120.2, 118.5, 112.0, 165.7 (OCO)
76	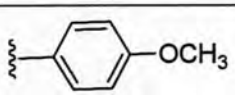	7.55 (2H, d, 8.8), 6.77 (2H, d, 8.8)	163.2, 131.3 (2C), 121.4, 113.7 (2C), 164.9 (OCO)
77	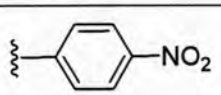	8.17 (2H, d, 8.5), 7.80 (2H, d, 8.5)	150.5, 134.2, 130.4 (2C), 123.6 (2C), 163.6 (OCO)
78	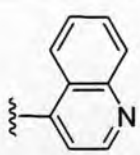	8.90 (1H, d, 4.3), 8.58 (1H, d, 8.3), 8.16 (1H, d 8.3), 7.77 (1H, t, 8.3), 7.57 (1H, t, 8.3), 7.49 (1H, d, 4.3)	149.4, 149.1, 133.4, 130.2, 130.1, 128.6, 125.4, 124.7, 122.0, 165.1 (OCO)
79	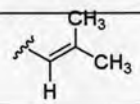	5.21 (1H, br s), 1.92 (3H, s), 1.71 (3H, s)	157.7, 115.2, 27.3, 20.1, 165.7 (OCO)
80	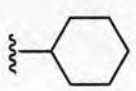	1.88 (1H, overlap), 1.55 (2H, m), 1.52 (2H, m), 1.50 (2H, m), 1.01 (2H, m), 1.00 (2H, m)	43.1, 29.2, 28.8, 25.6, 25.4, 25.3, 175.2 (OCO)

2.2.2 22-*O*- alicyclic acyl renieramycin analogs

The HR-EIMS data of all alicyclic acyl renieramycin analogs were shown in Table 18. The UV spectra of analogs displayed the quinone absorption at λ_{max} at 269-270 nm. The IR absorption spectra of alicyclic acyl analogs showed bands at 1615, 1652 cm^{-1} (C=O stretching), implying the quinone character and absorption band at 1714-1731 cm^{-1} implying the ester carbonyls. Most of alicyclic acyl renieramycin analogs showed absorption band at 2228 cm^{-1} which was a cyano group (CN) at C-21 excepting analog **80** containing a hydroxyl group at this position. The protons and carbons assignments were performed by 1D-NMR and 2D-NMR, including ^{1}H-^{1}H COSY, HMQC, HMBC, and NOESY and compared with NMR data of deangeloylrenieramycin M. In general, the 500 MHz ^{1}H NMR and 125 MHz ^{13}C NMR spectra in $CDCl_3$ of all alicyclic acyl renieramycin analogs showed signals similar to those of acyclic acyl renieramycin analogs except the difference of the side chains at C-22. From the 500 MHz ^{1}H NMR and 125 MHz ^{13}C NMR, the side chains of analogs **68** and **69** showed a group of methine proton at δ 2.36 ppm and 1.91 ppm, respectively. Other protons of the side chains of analogs **68** and **69** were methylene protons (δ 1.59-1.04 ppm). Analogs **70-73** revealed methylene protons and olefinic protons as shown in Table 19. Olefinic protons of analogs **70** and **72** (δ ~ 6.50 ppm) showed more downfield signals than those of analogs **71** and **73** (δ ~ 5.40-5.80 ppm). These results indicated that olefinic protons of analogs **70** and **73** were β proton of the α, β unsaturated esters. Proton chemical shift at C-21 of analog **80** (δ 4.38 ppm) shifted more downfield than analog **69** (δ 4.00 ppm) about 0.38 ppm. The result showed that C-21 of analog **80** connected to an oxygen atom. Carbon chemical shift of analog **80** at C-21 showed downfield at δ 82.4 ppm more than analog **69** (δ 58.7 ppm). Analogs **68**, **69**, **71**, **73** and **80** revealed sp^3 methine carbon (δ ~ 43-44 ppm), methylene carbon (δ ~ 20-35 ppm). Analogs **71** and **73** showed olefinic carbons of the isolated double bond at δ ~ 120-129 ppm. Analogs **70** and **72**, which contained an α, β unsaturated esters showed α-carbons at 134.8 ppm, and 129.6 ppm and β carbons at 144.7 ppm, and 140.6 ppm, respectively. Interestingly, the ester carbonyl carbons at 22-*O*-acyl of alicyclic acyl renieramycin analogs shifted downfield at δ ~175 ppm comparable to conjugated alicyclic acyl renieramycin analogs (δ ~165). Analog **73** was obtained as a mixture of diastereoisomers since the corresponding acid anhydride used was an enantiomeric mixture. The ^{1}H NMR of analog **73** clearly showed pairs signals of 22-Ha at δ 4.28 ppm (minor isomer) and ppm 4.35 ppm (major isomer); 22-

Hb at δ 4.00 ppm (major isomer) and 4.06 (minor isomer). In addition, the ^{13}C NMR of analog **73** also showed pairs signals of C-9 at δ 135.45 ppm (major isomer) and 135.50 ppm (minor isomer); C-19 at δ 135.10 ppm (major isomer) and 135.11 ppm (minor isomer). The ratio of major and minor isomer was 6:5.

2.2.3 22-*O*- aromatic acyl renieramycin analogs

The HR-EIMS and HR-FABMS data of all analogs **74-78** were shown in Table 18. The UV spectra of all analogs exhibited λ_{max}) at 258-270 nm. The IR spectra of analogs **74-78** were showed in Figures 145, 150, 155, 161, and 166. The 500 MHz ^1H NMR and 125 MHz ^{13}C NMR spectra of all analogs are similar to that of deangeloylrenieramycin M. The NMR spectral data of analogs **74-78** were different only the side chains at C-22 as shown in Table 19. Analog **74** containing the benzoate side chain at C-22 showed the pattern of proton signals at δ 7.60 (1H, dd, J = 7.7, 1.2 Hz, 2'-H and 6'-H), 7.50 (1H, dt, J = 7.7, 1.6 Hz, 4'-H), 7.31 (1H, t, J = 7.7 Hz, 3'-H and 5'-H) and carbon signals at δ 133.1 (C-4'), 130.0 (C-1'), 129.2 (C-2' and C-6'), 128.4 (C-3'and C-5'). The ^1H NMR and ^{13}C NMR spectra of analogs **75** and **76** showed the signals attributable to the phenyl protons and carbons in the range of δ_H 8-6 ppm and in the range of δ_C164-113 ppm, respectively. Both analogs also showed a singlet proton signal and a carbon signal of an aryl methoxy group at δ 3.62 ppm and 55.6 ppm (2'-OCH_3) and δ 3.81 ppm and 55.5 ppm (4'-OCH_3), respectively. The downfield quaternary carbon signals at δ 158.5 ppm (C-2') of analog **75** and δ 163.2 ppm (C-4') of analog **76** were assigned to oxygenated sp^2 carbons. Analog **77** showed two doublets of aromatic protons at 8.17 ppm (2H, d, J = 8.5 Hz, 3'-H and 5'-H) and 7.80 ppm (2H, d, J = 8.5 Hz, 2'-H and 6'-H) and four olefinic methine carbons appeared at δ 130.4 ppm (C-2' and C-6') and 123.6 ppm (C-3' and C-5'). At C-4' of analog **77** was substituted with NO_2. The HR-FABMS of analog **78** showed $[M+H]^+$ ion peak at *m/z* 649.2296 corresponding to the molecular formula $C_{36}H_{32}N_4O_8$. Analog **78** was quinoline acylated product. The proton signals of quinoline showed at δ 8.90 (1H, d, J = 4.3 Hz, 2'-H), 8.58 (1H, d, J = 8.3 Hz, 5'-H), 8.16 (1H, d, J = 8.3 Hz, 8'-H), 7.77 (1H, t, J = 8.3 Hz, 7'-H), 7.57 (1H, t, J = 8.3 Hz, 6'-H), 7.49 (1H, d, J = 4.3 Hz, 3'-H) and carbon signals at δ 149.4 ppm (C-2'), 149.1 ppm (C-8'a), 133.4 ppm (C-4'), 130.2 ppm (C-7'), 130.1 ppm (C-8'), 128.6 ppm (C-6'), 125.4 ppm (C-5'), 124.7 ppm (C-4'a), 122.0 ppm (C-3'). Interestingly, the NOESY experiment of analogs **76**

(Figure 158) and **78** (Figure 163) showed correlations of 2'-H and 6'-H to 4-Hβ and 3'-H to 4-Hβ, respectively. This information revealed the orientation of the aromatic acyl chains of both renieramycin analogs were paralleled to the quinone ring E. Therefore, the aromatic affected to the upfield-shifts of the protons of 17-OCH_3 (δ 3.71 ppm and 3.65 ppm) and 16-CH_3 (δ 1.72 ppm and 1.16 ppm).

2.3 Cytotoxic activity of renieramycin analogs

All renieramycin analogs were evaluated *in vitro* for cytotoxicity by measuring cell growth inhibition with a cell counting kit (DOJINDO, Osaka, Japan) against three human carcinoma cell lines including, HCT116 (colon carcinoma), QG56 (lung carcinoma), and DU145 (prostate carcinoma) as summarized in Table 20. The cytotoxicity was also determined by MTT colorimetric assay against HCT116 (colon) and MDA-MB-435 (breast) as shown in Table 21. The cytotoxicity results from a cell counting kid (Dojindo) demonstated that most analogs showed much less cytotoxicity than the parent renieramycin M except short-branched acyclic **64**, α, β unsaturated aliphatic carbonyl **67**, **70**, and aromatic **76** and **77** acyl derivatives expressed cytotoxic potency against DU145 similar to renieramycin M. Long chain acyclic acyl derivatives **65** and **66** dramatically lost cytotoxicity. The alicyclic five-membered ring acyl derivatives **68**, **70** and **71** showed more cytotoxicity than the alicyclic six-membered ring acyl derivatives **69**, **72** and **73**. The reduction in cytotoxicity might be due to steric hindrance. Analogs **79** and **80** containing hydroxyl group at C-21 showed also high cytotoxicity. Therefore, either 21-OH or 21-CN is essential for cytotoxic activity. Moreover, jorunnamycin A or deangeloylrenieramycin M was less potent than renieramycin M. This information supports that the ester side chain at C-22 is required for potent cytotoxicity of the marine bistetrahydroisoquinolines. The cytotoxicity results from the MTT assay are similar to those obtained by using the cell counting kit (Dojindo). In addition, the quinoline analog **78** revealed the same potent cytotoxicity when compared with renieramycin M. However, these cytotoxic results of renieramycin analogs are the important information to study more derivatives in the future.

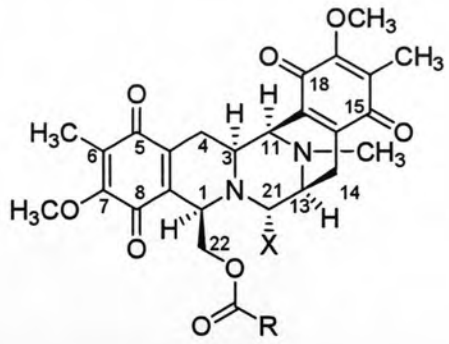

Table 20 Cytotoxicity of renieramycin analogs used a Dojindo cell counting kit.

Analog	R	X	IC_{50} (nM)		
			HCT 116	QG56	DU145
Renieramycin M	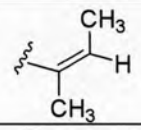	CN	9.8	24	2.1
Deangeloyl-renieramycin M	22-OH	CN	13.0	9.0	29.0
60	H	CN	NT	NT	NT
Cyanojorumycin	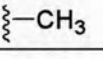	CN	<0.38	0.68	<0.38
Jorunnamycin C	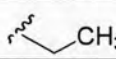	CN	1.5	2.8	0.32
61	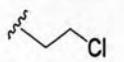	CN	NT	NT	NT
62	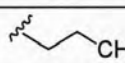	CN	24	37	5.8
63	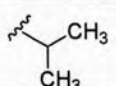	CN	NT	NT	NT
64	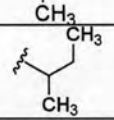	CN	22	38	2.2
65		CN	52	120	19
66		CN	110	150	33
67	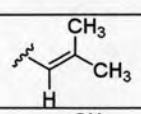	CN	14	32	2.4
79	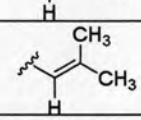	OH	9.0	34	7.2
68	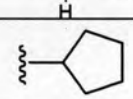	CN	51	130	9.5

NT = not tested

Table 20 (continued).

Analog	R	X	IC_{50} (nM)		
			HCT 116	QG56	DU145
69	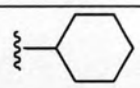	CN	130	170	25
80	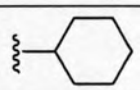	OH	13	48	9.6
70	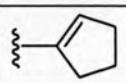	CN	24	37	2.7
71	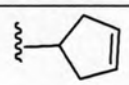	CN	31	44	4.1
72	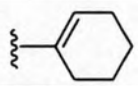	CN	41	120	9.4
73	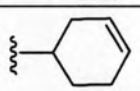	CN	47	130	8.6
74	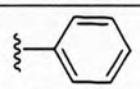	CN	14	53	5.2
75	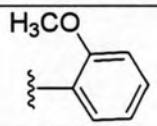	CN	16	59	5.2
76	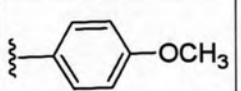	CN	5.0	18	1.6
77		CN	8.8	24	3.5
78	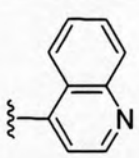	CN	NT	NT	NT

NT = not tested

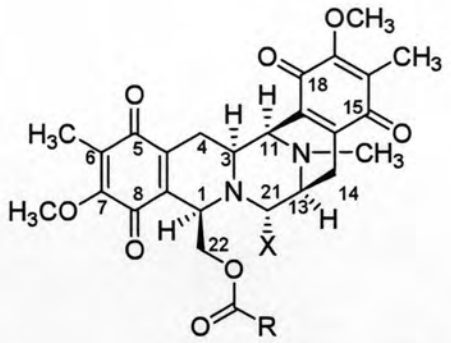

Table 21 Cytotoxicity of renieramycin analogs used MTT assay.

Analog	R	X	IC_{50} (nM)	
			HCT 116	MDA-MB-435
Renieramycin M	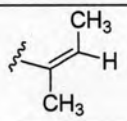	CN	11 ± 0.59	4.2 ± 0.28
Deangeloyl-renieramycin M	22-OH	CN	120 ± 8.1	290 ± 4.4
60	H	CN	38 ± 1.9	38 ± 1.6
Cyanojorumycin	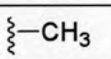	CN	10 ± 0.53	9.8 ± 0.44
Jorunnamycin C	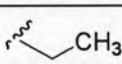	CN	27 ± 0.95	16 ± 1.3
61	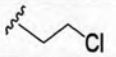	CN	16 ± 0.70	12 ± 0.47
62	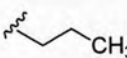	CN	34 ± 1.4	12 ± 2.41
63	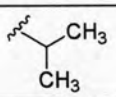	CN	22 ± 1.5	10 ± 0.12
64	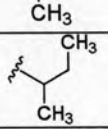	CN	33 ± 0.89	12 ± 0.30
65		CN	100 ± 2.4	40 ± 0.63
66	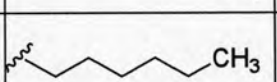	CN	NT	NT
67	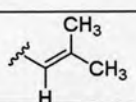	CN	27 ± 2.3	11 ± 0.31
79	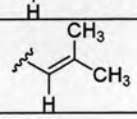	OH	NT	NT
68	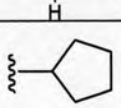	CN	93 ± 5.2	30 ± 0.51
69	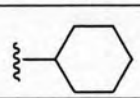	CN	NT	NT

NT = not tested

Table 21 (continued).

Analog	R	X	IC_{50} (nM)	
			HCT 116	**MDA-MB-435**
80	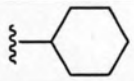	OH	NT	NT
70	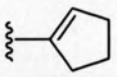	CN	33 ± 2.2	13 ± 0.70
71	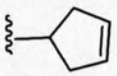	CN	33 ± 1.1	13 ± 0.72
72	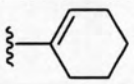	CN	49 ± 2.0	29 ± 0.26
73	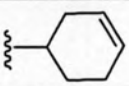	CN	43 ± 0.74	27 ± 3.1
74	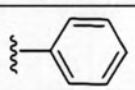	CN	NT	NT
75	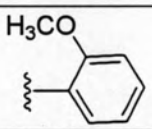	CN	NT	NT
76	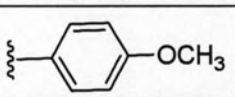	CN	NT	NT
77		CN	NT	NT
78	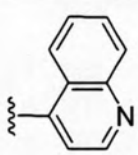	CN	10 ± 0.33	4.1 ± 0.095

NT = not tested

3. DNA microarray

Renieramycin M and jorunnamycin C were isolated from the KCN-pretreated sponge, *Xestospongia* sp. and the nudibranch, *Jorunna funebris*, respectively. Both compounds, containing different side chains at the C22 ester part, have been reported to show potent cytotoxicity against several cancer cell lines in low nM concentrations. To examine the effects of renieramycin M and jorunnamycin C on transcription, the author carried out oligonucleotide microarray analysis with particular focus on the similarity and difference between both compounds in terms of their transcriptional profiles.

3.1 *In vitro* antiproliferative activity

After 3 day continuous drug exposure, the drug concentration required for 50% growth inhibition (IC_{50}) was determined by the MTT colorimetric assay. The results are presented in Table 22. In this assay system, renieramycin M was more active than jorunnamycin (about 2 folds on the IC_{50} basis) against both HCT116 colon and MDA-MB-435 breast cancer cell lines.

Table 22 *In vitro* antiproliferative activity of renieramycin M and jorunnamycin C.

Compound	Human cancer cell line, $IC_{50} \pm$ SD (nM)	
	HCT116 (colon)	MDA-MB-435 (breast)
Renieramycin M	16 ± 0.34	6.3 ± 0.065
Jorunnamycin C	27 ± 0.95	16 ± 1.3

3.2 Microarray-based transcription profiling of renieramycin M and jorunnamycin C

In order to compare renieramycin M and jorunnamycin C on the basis of their transcriptional effects, we analyzed expression changes of more than 8,500 genes in HCT116 and MDA-MB-435 cells using Affymetrix Human Genome Focus arrays. The investigated time points were 4 h and 12 h. All the data were taken in triplicate to verify statistical significance. Shown in Figure 3 are the hierarchical clustering data on the dendrogram format and cosine coefficients between any two data points on the table format. In this analysis, renieramycin M and jorunnamycin C were shown to have similar transcriptional effects on each human cancer cell line and also at each

time point (cosine coefficients: 0.66 in the 4 h treatment for HCT116; 0.57 in the 12 h treatment for HCT116; 0.74 in the 4 h treatment for MDA-MB-435; and 0.76 in the 12 h treatment for MDA-MB-435). The observed high correlation indicates that both compounds share the same primary mechanism(s) of action particularly in MDA-MB-435, a more sensitive cell line to these cytotoxic.

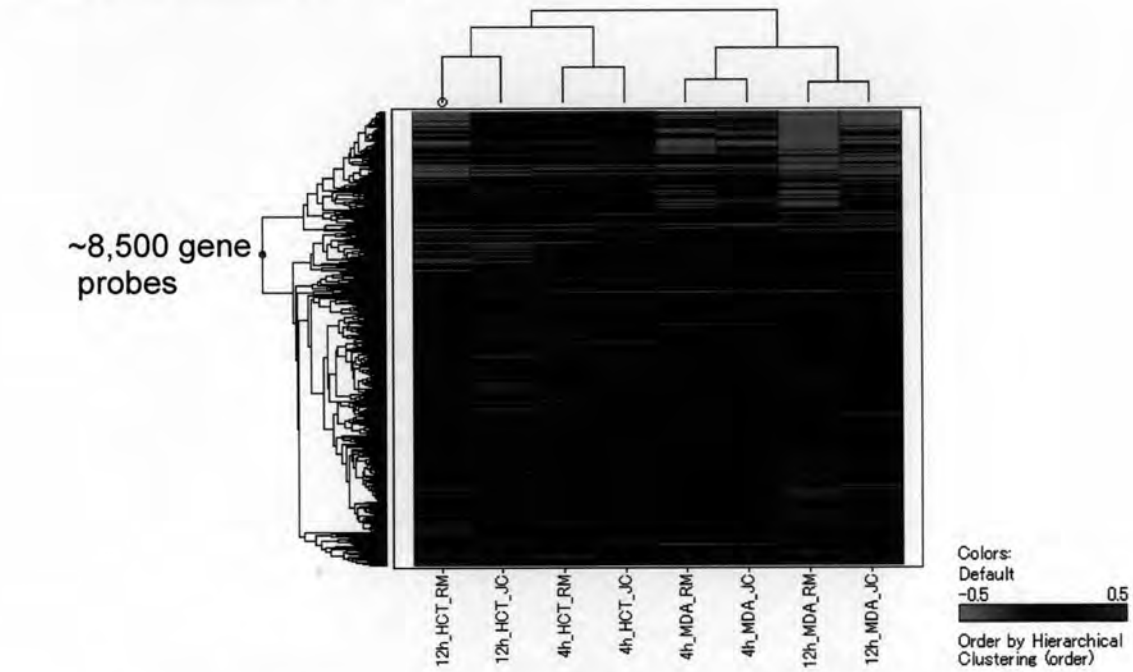

	4h_HCT_RM	4h_HCT_JC	4h_MDA_RM	4h_MDA_JC	12h_HCT_RM	12h_HCT_JC	12h_MDA_RM	12h_MDA_JC	
4h_HCT_RM	1.00	0.66	0.21	0.32	0.41	0.44	0.18	0.24	4h_HCT_RM
4h_HCT_JC	0.66	1.00	0.12	0.19	0.29	0.30	0.12	0.15	4h_HCT_JC
4h_MDA_RM	0.21	0.12	1.00	[illegible]	0.34	0.00	0.65	0.44	4h_MDA_RM
4h_MDA_JC	0.32	0.19	[illegible]	1.00	0.41	0.20	0.50	0.46	4h_MDA_JC
12h_HCT_RM	0.41	0.29	0.34	0.41	1.00	0.57	0.50	0.59	12h_HCT_RM
12h_HCT_JC	0.44	0.30	0.00	0.20	0.57	1.00	[illegible]	0.18	12h_HCT_JC
12h_MDA_RM	0.18	0.12	0.65	0.50	0.50	[illegible]	1.00	[illegible]	12h_MDA_RM
12h_MDA_JC	0.24	0.15	0.44	0.46	0.59	0.18	[illegible]	1.00	12h_MDA_JC

Figure 3 Hierarchical clustering data of renieramycin M (RM) and jorunnamycin C (JC).

Venn diagrams in Figure 4 present the number of genes up- and down-regulated at least 2-fold with statistical significance ($p < 0.05$) by treatment with renieramycin M and jorunnamycin C. The obtained results can be summarized as follows: (i) transcriptional down-regulation was predominant over up-regulation for both compounds irrespective of the cell lines and the time points in general; (ii) the numbers of significantly altered genes by renieramycin M and jorunnamycin C treatments were more in MDA-MB-435 than in HCT116, consistent with the order of cellular sensitivity to both compounds; (iii) significant overlap was observed between

the altered genes by renieramycin M and jorunnamycin C treatments in both cell lines; and (iv) the numbers of significantly altered genes in both cell lines were more in renieramycin M treatment than in jorunnamycin C treatment, even though the drug concentrations for this analysis were corrected by using the 2 x IC_{50}s for both compounds.

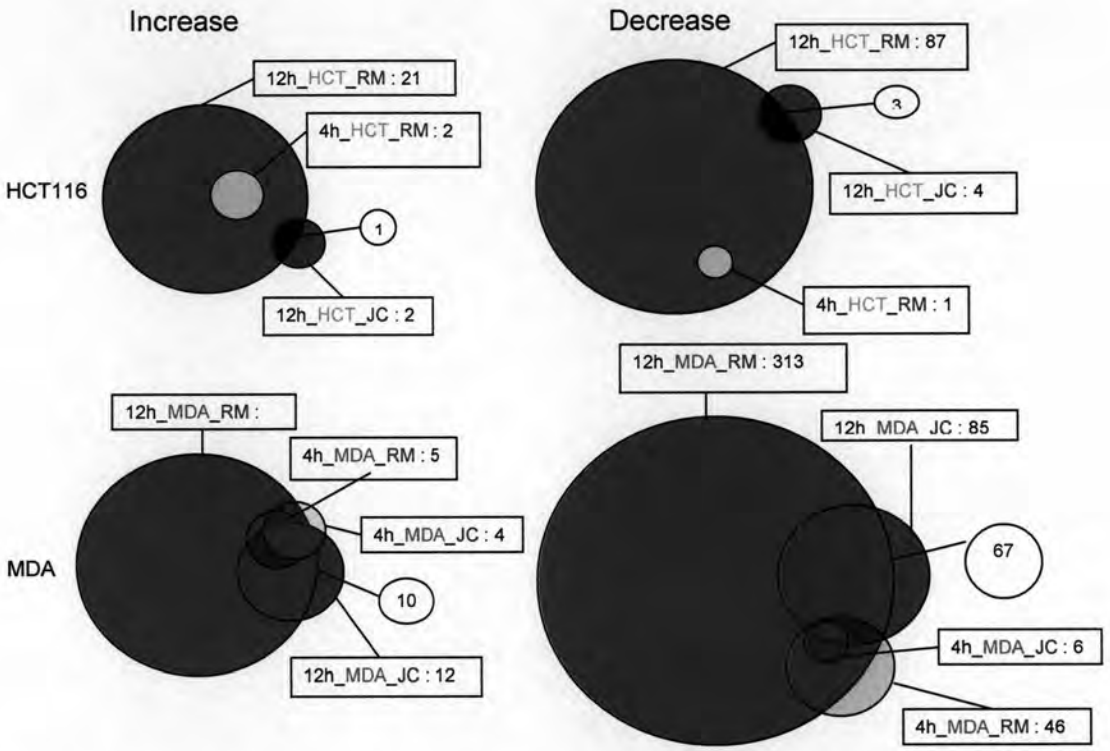

Figure 4 Venn diagrams comparing set of up-and down-regulated genes in HCT116 colon and MDA-MB-435 breast cancer cells treatment with each of renieramycin M (RM) and jorunnamycin C (JC).

Figure 5 highlights the genes significantly altered by 12 h treatments with renieramycin M and jorunamycin C in common in HCT116 and MDA-MB-435. In this analysis, 37 genes were found to be down-regulated by renieramycin M (at 2 x IC_{50}s for 12 h) in common in both cell lines, subjected to GO analysis to examine compound-associated biological processes, cellular components, and molecular functions. As a result, the following GO terms were illuminated as profoundly related to renieramycin M treatment: cell division in biological processes; intercellular junction in cellular components; and diacylglycerol binding in molecular functions. It should be mentioned that the relation between renieramycin M treatment and cell

division appears to be well consistent with the compound-induced G_2-M arrest phenotype in cell cycle analysis (data not shown).

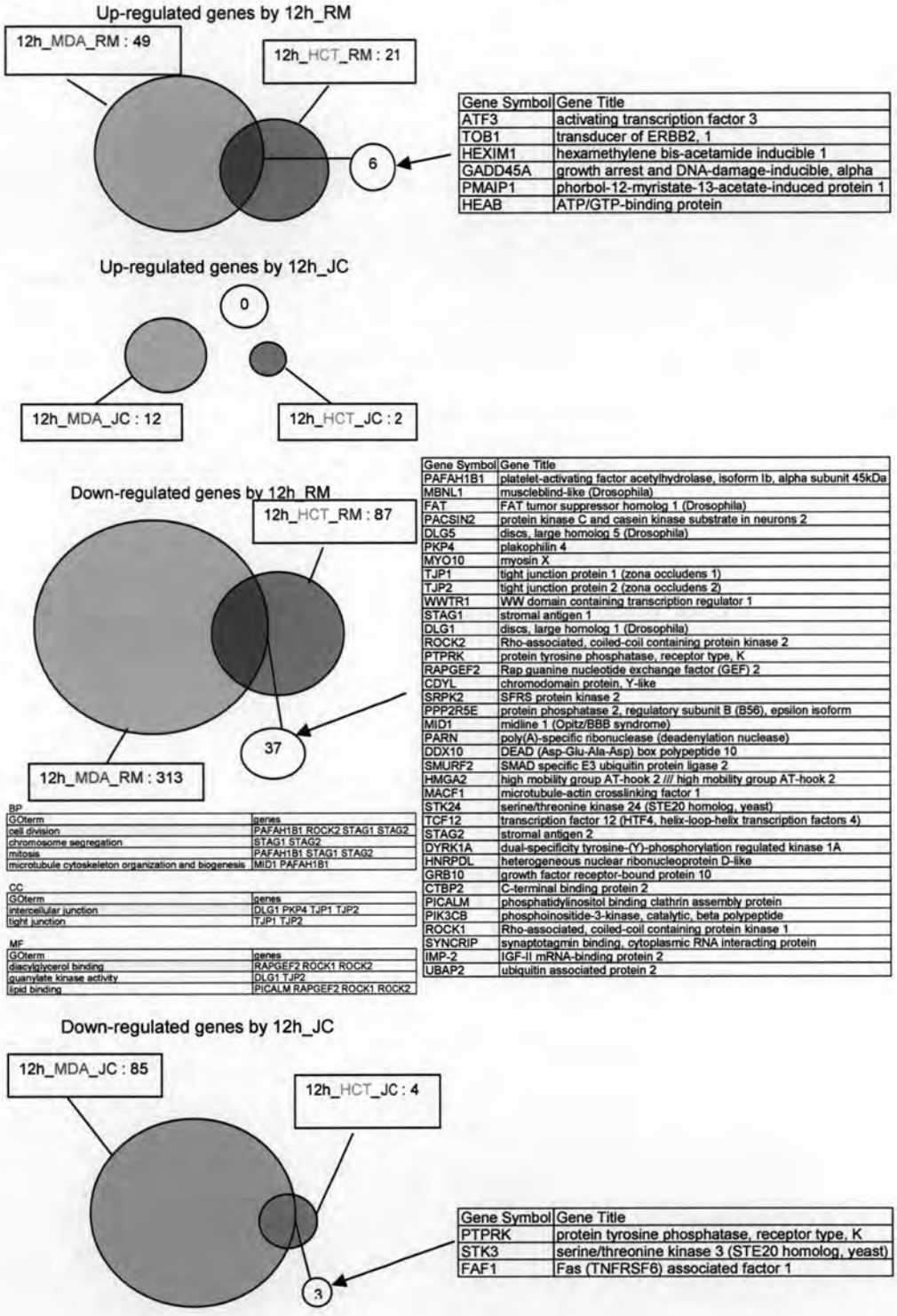

Gene Symbol	Gene Title
ATF3	activating transcription factor 3
TOB1	transducer of ERBB2, 1
HEXIM1	hexamethylene bis-acetamide inducible 1
GADD45A	growth arrest and DNA-damage-inducible, alpha
PMAIP1	phorbol-12-myristate-13-acetate-induced protein 1
HEAB	ATP/GTP-binding protein

Gene Symbol	Gene Title
PAFAH1B1	platelet-activating factor acetylhydrolase, isoform Ib, alpha subunit 45kDa
MBNL1	muscleblind-like (Drosophila)
FAT	FAT tumor suppressor homolog 1 (Drosophila)
PACSIN2	protein kinase C and casein kinase substrate in neurons 2
DLG5	discs, large homolog 5 (Drosophila)
PKP4	plakophilin 4
MYO10	myosin X
TJP1	tight junction protein 1 (zona occludens 1)
TJP2	tight junction protein 2 (zona occludens 2)
WWTR1	WW domain containing transcription regulator 1
STAG1	stromal antigen 1
DLG1	discs, large homolog 1 (Drosophila)
ROCK2	Rho-associated, coiled-coil containing protein kinase 2
PTPRK	protein tyrosine phosphatase, receptor type, K
RAPGEF2	Rap guanine nucleotide exchange factor (GEF) 2
CDYL	chromodomain protein, Y-like
SRPK2	SFRS protein kinase 2
PPP2R5E	protein phosphatase 2, regulatory subunit B (B56), epsilon isoform
MID1	midline 1 (Opitz/BBB syndrome)
PARN	poly(A)-specific ribonuclease (deadenylation nuclease)
DDX10	DEAD (Asp-Glu-Ala-Asp) box polypeptide 10
SMURF2	SMAD specific E3 ubiquitin protein ligase 2
HMGA2	high mobility group AT-hook 2 /// high mobility group AT-hook 2
MACF1	microtubule-actin crosslinking factor 1
STK24	serine/threonine kinase 24 (STE20 homolog, yeast)
TCF12	transcription factor 12 (HTF4, helix-loop-helix transcription factors 4)
STAG2	stromal antigen 2
DYRK1A	dual-specificity tyrosine-(Y)-phosphorylation regulated kinase 1A
HNRPDL	heterogeneous nuclear ribonucleoprotein D-like
GRB10	growth factor receptor-bound protein 10
CTBP2	C-terminal binding protein 2
PICALM	phosphatidylinositol binding clathrin assembly protein
PIK3CB	phosphoinositide-3-kinase, catalytic, beta polypeptide
ROCK1	Rho-associated, coiled-coil containing protein kinase 1
SYNCRIP	synaptotagmin binding, cytoplasmic RNA interacting protein
IMP-2	IGF-II mRNA-binding protein 2
UBAP2	ubiquitin associated protein 2

BP

GOterm	genes
cell division	PAFAH1B1 ROCK2 STAG1 STAG2
chromosome segregation	STAG1 STAG2
mitosis	PAFAH1B1 STAG1 STAG2
microtubule cytoskeleton organization and biogenesis	MID1 PAFAH1B1

CC

GOterm	genes
intercellular junction	DLG1 PKP4 TJP1 TJP2
tight junction	TJP1 TJP2

MF

GOterm	genes
diacylglycerol binding	RAPGEF2 ROCK1 ROCK2
guanylate kinase activity	DLG1 TJP2
lipid binding	PICALM RAPGEF2 ROCK1 ROCK2

Gene Symbol	Gene Title
PTPRK	protein tyrosine phosphatase, receptor type, K
STK3	serine/threonine kinase 3 (STE20 homolog, yeast)
FAF1	Fas (TNFRSF6) associated factor 1

Figure 5 Venn diagrams comparing the common genes significantly altered by 12 h treatment with renieramycin M (RM) and jorunnamycin C (JC) in HCT116 and MDA-MB-435 cell lines.

Illustrated in Figure 6 is the candidate biomarker gene selection for the tetrahydroisoquinoline class of anticancer agents including renieramycin M and jorunnamycin C. The analysis was performed to search for genes significantly down-regulated in common in HCT116 and MDA-MB-435 as well as in common in renieramycin M and jorunnamycin C treatments. Finally, only one gene PTPRK (protein tyrosine phosphatasegene, receptor type, K) was found as satisfying the selection criteria. This gene might be used as a relevant biomarker to support drug efficacy to cancer cells.

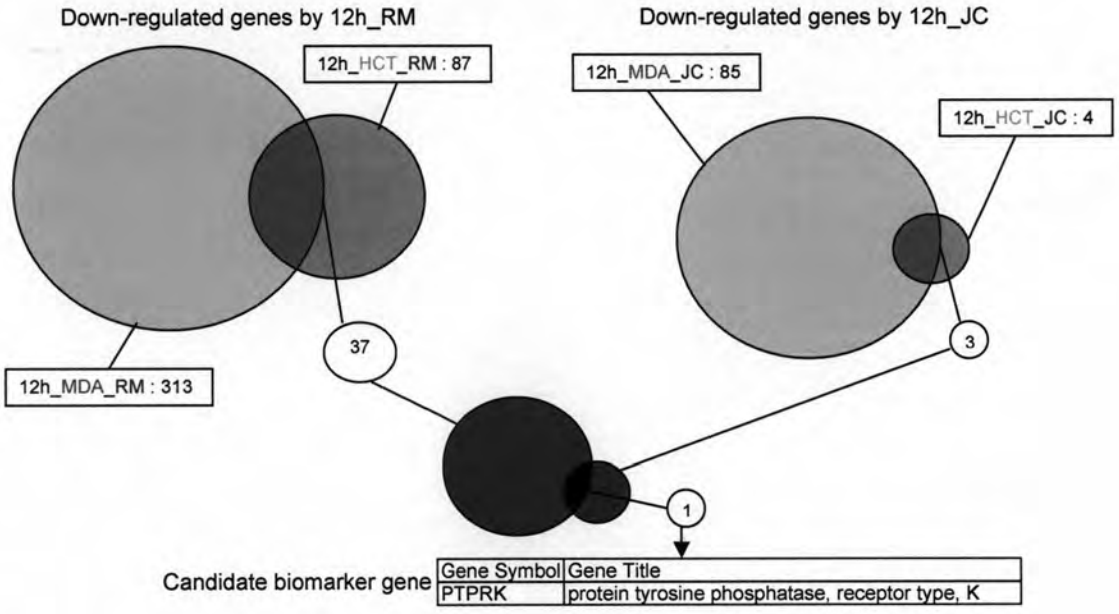

Figure 6 Venn diagrams comparing common down regulated gene altered by 12 h treatment with renieramycin M (RM) and jorunnamycin C (JC) in HCT116 and MDA-MB-435 cell lines.